Influence of cell-cell contact between L. thermotolerans and S. cerevisiae on yeast interactions and the exo-metabolome

Clément Petitgonnet, Géraldine Klein, Chloé Roullier-Gall, Philippe Schmitt-Kopplin, Beatriz Quintanilla-Casas, Stefania Vichi, Diane Julien-David, Hervé Alexandre

Influence of cell-cell contact between *L. thermotolerans* and *S. cerevisiae* on yeast interactions and the exo-metabolome.

Clément Petitgonnet[a], Géraldine L. Klein[a], Chloé Roullier-Gall[a], Philippe Schmitt-Kopplin[bc], Beatriz Quintanilla-Casas[d], Stefania Vichi[d], Diane Julien-David[e], and Hervé Alexandre[a*]

[a] *UMR Procédés Alimentaires et Microbiologiques, Equipe VAlMiS (Vin, Aliment, Microbiologie, Stress), AgroSup Dijon – Université de Bourgogne Franche-Comté, Institut Universitaire de la Vigne et du Vin, rue Claude LADREY, BP 27877, 21000 DIJON, France*

[b] *Helmholtz Zentrum Muenchen, Research unit Analytical BioGeoChemistry, Ingolstaedter Landstrasse 1, 85764 Neuherberg, Germany*

[c] *Technische Universität Muenchen, Analytical Food Chemistry, Alte Akademie 10, 85354 Freising, Germany*

[d] *Nutrition, Food Science and Gastronomy Department, INSA - XaRTA (Catalonian Reference Network on Food Technology), University of Barcelona, Santa Coloma de Gramenet, Spain*

[e] *Université de Strasbourg, CNRS, IPHC UMR 7178, F-67000 Strasbourg, France.*

*: corresponding author rvalex@u-bourgogne.fr

Summary:

Sequential fermentation of grape must inoculated with *L. thermotolerans* and then *S. cerevisiae* 24 h later (typical wine-making practice) was conducted with or without cell-cell contact between the two yeast species. We monitored cell viability of the two species throughout fermentation by flow cytometry. The cell viability of *S. cerevisiae* decreased under both conditions, but the decrease was greater if there was cell-cell contact. An investigation of the nature of the interactions showed competition between the two species for nitrogen compounds, oxygen, and must sterols. Volatile-compound analysis showed differences between sequential and pure fermentation and that cell-cell contact modifies yeast metabolism, as the volatile-compound profile was significantly different from that of sequential fermentation without cell-cell contact. We further confirmed that cell-cell contact modifies yeast metabolism by analyzing the exo-metabolome of all fermentations by FT-ICR-MS analysis. These analyses show specific metabolite production and quantitative metabolite changes associated with each fermentation condition. This study shows that cell-cell contact not only affects cell viability, as already reported, but markedly affects yeast metabolism.

Keywords: interactions, *S. cerevisiae*, *L. thermotolerans*, cell-cell contact, flow cytometry, metabolomics.

I. Introduction

Alcoholic fermentation in grape must is mainly performed by the well-known yeast *Saccharomyces cerevisiae*. However, *S. cerevisiae* is not the only yeast present on grape berries and in grape must. Other interesting yeasts, called non-*Saccharomyces*, are increasingly being studied because of their ability to improve the complexity of the wine aroma by increasing the concentration of certain aromatic molecules, such as terpenoids or higher alcohols (Ciani, 1997; Esteve-Zarzoso et al., 1998; Rojas et al., 2001; Jolly et al., 2006; Fleet, 2008; Benito, 2018; Zhang et al., 2018), or other molecule of interest, such as glycerol (Romano et al., 1992; Barbosa et al., 2015). The production of these molecules is mostly due to enzymatic activities present in non-*Saccharomyces* yeasts, which are lower or absent from *S. cerevisiae* strains (Esteve-Zarzoso et al., 1998; Strauss et al., 2001; Jolly et al., 2014). *Lachancea thermotolerans (L. thermotolerans)* is naturally present in grape must (Torija et al., 2001; Kapsopoulou et al., 2005) and has been reported to enhance the overall acidity of wine due to the high production of L-lactic acid (Mora et al., 1990; Gobbi et al., 2013). This characteristic may be desirable for wine with a low acidity (Balikci et al., 2016). Moreover, *L. thermotolerans* is able to increase the concentration of interesting aromatic molecules in co-fermentation with *S. cerevisiae* than when *S. cerevisiae* is used alone. These molecules include ethyl esters and terpenes (Benito et al., 2015; Balikci et al., 2016; Benito et al., 2016), as well as glycerol (Kapsopoulou et al., 2006). The biotechnological interest of co-fermentation with non-*Saccharomyces* and *S. cerevisiae* in wine making is now clear (García et al., 2016), but co-fermentation is not well controlled. Indeed, the presence of non-*Saccharomyces* yeasts with *S. cerevisiae* during alcoholic fermentation leads to interactions between these different species (Ciani et al., 2016) which are highly dependent on the species and strains used (Wang et al., 2016). Among such interactions, competition for nutrients, such as nitrogen and oxygen, can be among the earliest that occur during co-fermentation, especially in sequential fermentations (inoculation with *S. cerevisiae* a minimum of 24 h after inoculation with the non-*Saccharomyces* yeast). Indeed, the non-*Saccharomyces* consume nutrients before *S. cerevisiae* inoculation, leading sometimes to sluggish fermentation (Sablayrolles et al., 1996; Alexandre and Charpentier, 1998; Taillandier et al., 2007). Among these nutrients, phytosterols may be good candidates to study these interactions. Indeed, under conditions of aerobiosis, yeast are able to synthesize unsaturated fatty acids (UFA) and sterols

for membrane integrity and energy production, with a succession of reactions involving oxygen-dependent enzymes (Tehlivets et al., 2007). However, in the absence of oxygen, these enzymes are not active and yeast use the fatty acids and sterols present in the must (Salmon, 2006). It is important to know the proportion of the phytosterols consumed by non-*Saccharomyces* before inoculation with *S. cerevisiae* when performing sequential fermentation.

Competition for nutrients is not the only interaction that occurs during alcoholic fermentation, because direct physical contact between non-*Saccharomyces* and *S. cerevisiae* cells could lead to cell-cell interactions. Indeed, several studies have shown early growth arrest of *Lachancea thermotolerans* in co-fermentations with *S. cerevisiae*. They concluded that this is due to a cell-cell contact mechanism (Nissen and Arneborg, 2003; Nissen et al., 2003), whereas Albergaria *et al.* (2009) and Branco *et al.* (2014) showed that antimicrobial peptide secretion is responsible for the early death of this non-*Saccharomyces* yeast. Several other molecules are involved in yeast-yeast interactions and affect the growth of yeast, such as tyrosol, tryptophol, and phenylethanol, which are *quorum sensing* molecules, especially under nitrogen-limiting conditions (Zupan et al., 2013; González et al., 2018; Valera et al., 2019). Additional interaction mechanisms have been reported and reviewed recently (Liu et al., 2015). Although cell-cell contact may explain some interactions between yeast, the effect of cell-cell contact on yeast metabolism relative to when the different species are physically separated has never been investigated.

Here, we exhaustively studied the interactions between *L. thermotolerans* and *S. cerevisiae* by comparing pure fermentations of each species with sequential fermentation, with and without their physical separation. The competition for yeast assimilable nitrogen (YAN), oxygen, and, for the first time, phytosterols was also studied. We analyzed the consequences of such interactions on volatile compound profiles and report, their impact on the exo-metabolome.

II. Materials and methods

1. Yeast strains

A modified *S. cerevisiae* strain supplied by INRA/SupAgro Montpellier was used in this study: *S. cerevisiae* 59A-GFP MATa ho *AMN1*::TEF2Pr-GFP-ADH1-NATMX4, a haploid derivative of the commercial wine strain EC1118, modified to strongly express eGFP(S65T) (Marsit et al., 2015).

L. thermotolerans BBMCZ7-FA20 (previously isolated and identified by Sadoudi et al. (2012)) was used as the non-*Saccharomyces* yeast strain.

2. Growth conditions

All yeast strains were grown at 28°C in modified YPD medium (20 $g.L^{-1}$ glucose, 10 $g.L^{-1}$ peptone, and 5 $g.L^{-1}$ yeast extract with 18 $g.L^{-1}$ of agar for Petri dish cultivation), supplemented with 0.1 $g.L^{-1}$ chloramphenicol. For fermentation inoculation, yeasts were pre-cultured in 250-mL sterile Erlenmeyer flasks, closed with dense cotton plugs, containing 150 mL modified YPD medium and incubated with agitation (100 rpm) at 28°C for 24 or 48 h.

3. Fermentation conditions

Fermentations were carried out in triplicate in white must containing 212.1 ± 4.81 $g.L^{-1}$ glucose/fructose, pH 3.41 ± 0.02, as well as 251.2 ± 20.5 $mg.L^{-1}$ total assimilable nitrogen. The must was centrifuged at 7,000 x g for 7 min at 4°C before use. Sugar concentration and ethanol production were monitored by Fourier transformed infra-red spectroscopy (FTIR, OenoFOSS™, FOSS, Hilleroed, Denmark). The detection cell was filled with 200 µL centrifuged (12,000 g for 5 min at 4°C) supernatant from cultures and the analysis run using FOSS User Interface software.

3.1. Pure fermentations

Pure fermentations were carried out in 1-L test tubes containing 800 mL white must and closed with specific silicon caps. Each test tube was inoculated with 10^6 $cells.mL^{-1}$ from a YPD-medium pre-culture of *S. cerevisiae* or *L. thermotolerans* and incubated at 20°C without agitation.

3.2. Sequential fermentations in flasks

Sequential fermentations were carried out in 2-L pasteurized (2 h at 70°C) test tubes, closed with specific silicon caps. Two different fermentation conditions were tested: without (i) and with (ii) cell-cell contact.

i. Three test tubes were filled with 1.2 L white must and a dialysis membrane (Spectra/por, Spectrum Labs, MWCO 12-14 kDa, diameter 48 mm, length 60 cm) containing 600 mL white must was added to each test tube (total must volume 1.8 L). The dialysis membranes were inoculated with 10^6 $cells.mL^{-1}$ *L. thermotolerans* from YPD pre-cultures, and the test tubes (external medium) inoculated 24 h later with 10^6 $cells.mL^{-1}$ of *S. cerevisiae* from a YPD pre-culture.

ii. Three test tubes were filled with 1.8 L white must (no dialysis membrane), inoculated with 10^6 cells.mL^{-1} *L. thermotolerans*, and then 24 h later with 10^6 cells.mL^{-1} *S. cerevisiae*, both from YPD pre-cultures.

All test tubes were incubated at 20°C without agitation.

4. Flow cytometric analysis

4.1. Yeast viability

All fluorescent dyes used in this study were purchased from ThermoFisher Scientific, Invitrogen.

Yeast viability was monitored during fermentation with propidium iodide (PI) dye (maximum excitation/emission wavelengths 538/617 nm), which binds to DNA when the cell membrane is compromised, triggering its fluorescence. Fermenting yeast (1 mL) was centrifuged at 12,000 x g for 5 min at 4°C. The pellet was resuspended in 1 mL PBS buffer (137 mM NaCl, 2.7 mM KCl, and 11.9 mM Phosphate, pH 7.2) (Fisher Scientific, Illkirch, France) and serial dilutions prepared. PI (1 µL at 0.1 mg.mL^{-1} in water) was added to a 100 µL aliquot. Samples were incubated 10 min in the dark and analyzed by flow cytometry.

4.2. Flow cytometer settings

Flow cytometry was performed with a BD Accuri C6 flow cytometer and the data analyzed using BD Accuri C6 software. For each run, 20 µL of sample was analyzed at 34 µL.min^{-1}, with a FSC threshold of 80,000, and SSC-H/FSC-H plots analyzed using logarithmic axes. A 488-nm wavelength argon laser was used to excite the cells (autofluorescence) and dye. An FL3-H long-pass filter (675 nm) was used for PI fluorescence.

5. Amino-acid and oxygen quantification

Oxygen consumption during alcoholic fermentation was monitored using Pst3 sensors (Nomacorc©) placed at the inner face at the top of the test tubes. The oxygen concentration was read using a NomaSense™ O2 P300 device (Nomacorc©), following the manufacturer's instructions. The oxygen concentration was measured in triplicate before stirring the media in the test tubes.

Amino acids and ammonium were quantified by HPLC as described previously (Gobert et al., 2017).

6. Phytosterol quantification by gas chromatography-mass spectrometry (GC-MS)

Must samples (50 mL) were taken at T0 and T24 h, corresponding to the must without yeast and 24 h of fermentation by *L. thermotolerans*, respectively. Prior to extraction, 250 µL of cholesterol (Sigma-Aldrich, Merck, Germany) at 1.0 $mg.mL^{-1}$ in ethyl acetate (Sigma-Aldrich, Merck, Germany) was added in must samples. Must samples were transferred to a separatory funnel, 25 mL of chloroform (Biosolve Chimie, France) added, the samples well agitated, and the organic lower phase collected. This step was repeated three times and the organic phases were combined. To eliminate remaining water, anhydrous sodium sulfate (Na_2SO_4 powder, Sigma-Aldrich, Merck, Germany) was added. Samples were transferred to 250 mL glass balloons and the solvent evaporated with a rotary vacuum evaporator to reduce the volume to approximately 1 mL. This volume was transferred to 1-mL brown-glass vials and completely evaporate under an N_2 flux. A cold saponification was done by adding 900 µL of absolute ethanol (Carlo Erba, France) and 250 µL of a saturated potassium hydroxide (KOH, Merck Darmstadt, Germany) aqueous solution into each vial. Samples were purged with nitrogen, and was put into a rotary shaker (Edmund Buhler, Johanna Otta GmbH, Hechingen, Germany) at ambient temperature in the dark overnight (15 h). The solution was transferred in a 100 mL separation funnel and 10 mL of distilled water were added. The unsaponifiable fraction was extracted three time with 2 mL of diethyl ether (Sigma-Aldrich, Merck KGaA, Darmstadt, Germany). The combined organic extracts were removed with a rotary vacuum evaporator and the residue was dried under nitrogen flow. After additional 2 mL of diethyl ether, the unsaponifiable residue was carefully transferred to a 2 mL glass test tube and then evaporated to dry matter under nitrogen flow. Then the sterol residue was converted to trimethylsilyl (TMS, Sigma-Aldrich, Merck, Germany) ethers with 100 µL of pyridine and 100 µL of N,O-Bis(trimethylsilyl)trifluoroacetamide (BSTFA, Sigma-Aldrich, Merck, Germany) at room temperature in the dark overnight and then, diluted with 800 µL of isooctane (Sigma-Aldrich, Merck, Germany). One microliter of each sample was injected into the GC–MS system. Phytosterol analyses were performed on a GC-MS device, composed of a Varian STAR 3400 GC instrument equipped with an “on-column” injector coupled to a mass spectrometer (Saturn 2000, Varian, France) with Electronic Impact as an ionization source (EI, ionization energy of 70 eV), working with a mass range from 40 to 600 m/z. Data acquisition and processing were performed with Varian Saturn Work Station 5.11 software using the NIST mass spectral database for compound identification. The separation of each compound was performed with a capillary column Factor Four VF-5ms (stationary phase: 5%

phenyl-95% dimethylpolysiloxane, thickness of 0.1 m, 60 m x 0.25 mm, Varian, France). Initial temperature of the column was 50°C (maintained for 2 min). The column temperature was programmed to reach 105°C at a rate of 7°C.min^{-1} (maintained for 2 min), then 170°C at a rate of 10°C.min^{-1} (maintained for 2 min), and finally 320°C at a rate of 7°C.min^{-1} (maintained for 15 min). The injector temperature was set to 50°C and programed to reach 300°C at a rate of 100°C.min^{-1} and kept at this temperature until the end of analysis. The injected volume was set to 1 µL and was under the control of an automatic injector (8500, Varian, France). The carrier gaz was Helium (99,9995%, Air liquid, France) and was set to a flow rate of 1 mL.min^{-1}. Sterols were quantified against cholesterol as an internal standard.

7. Volatile compound quantification

Volatile compounds were quantified by HeadSpace-Solid Phase MicroExtraction-Gas Chromatography/Mass Spectrometry as reported previously (Gobert et al., 2017). Briefly, 2 mL of wine was placed in a 10-mL vial fitted with a silicone septum, which was then transferred to a silicon oil bath at 40°C and the sample incubated for 10 min with magnetic stirring (700 rpm). A divinylbenzene/carboxen/polydimethylsiloxane (DVB/CAR/PDMS) fiber (Supelco, Bellefonte, PA, USA) was exposed to the sample headspace for 30 min and then subjected to immediate desorption in the gas chromatograph injector set at 260°C. Volatile compounds were analyzed by gas chromatography coupled to a quadrupolar mass-selective spectrometer. GC–MS analysis was performed in complete scanning mode (SCAN) in the 30–300 mass unit range. Compounds were identified by comparing their mass spectra and retention times with those of standard compounds or with those available in the Wiley 6 mass spectrum library or reported in previous publications.

8. Metabolomics: Fourier Transform-Ion Cyclotron Resonance-Mass Spectrometry (FT-ICR-MS)

8.1. FT-ICR-MS metabolome profiling

Direct-infusion FT-ICR mass spectra were acquired with a 12 Tesla Bruker Solarix FT-ICR mass spectrometer (Bruker Daltonics, Bremen, Germany). The samples were diluted 2:100 (v/v) in methanol (LC-MS grade, Fluka, Germany). Quality control (QC) samples were prepared by pooling equal amounts of all samples. QC samples were analyzed at the beginning and after every 10 samples to monitor the reproducibility of the measurements. QC spectra showed good repeatability and reproducibility of the method (spectrum profiles were very similar between each QC) with a very low coefficient of variation (supp fig. 1). The

diluted samples and QC samples were infused into the electrospray ion source at a flow rate of 2 µL.min^{-1}. Settings for the ion source were: drying gas temperature, 180°C; drying gas flow, 4.0 L.min^{-1}; capillary voltage, 3600 V. The spectra were acquired with a time-domain of 4 megawords and 300 scans were accumulated within a mass range of 92 to 1000 m/z. A resolving power of 400,000 at 300 m/z was achieved. Exported features were assigned to elemental formulae and represented using an H/C *vs.* O/C van Krevelen diagram, which highlights family compounds, such as carbohydrates (H/C 1.5-2; O/C 0.8-1), fatty acids (H/C 1.9-2.1; O/C 0-0.25), amino acids (H/C 1-2; O/C 0.2-0.8), nucleic acids (H/C 1.1-1.4; O/C 0.3-1), and anthocyanins (/C 0.5-1; O/C 0.4-0.8) (fig. 1). The metabolite formulae can then be entered into data bases, such as KEGG, Lipidmap, YMDB, Metlin, or an in-house developed plant and wine database, to annotate them and identify corresponding metabolic pathways.

8.2. Statistical analysis

The MS was first calibrated using arginine ion clusters (57 nmol.mL^{-1} in methanol). Next, raw spectra were further internally calibrated using a reference list, including known wine markers and ubiquitous fatty acids, to achieve the best possible mass accuracy and precision among the samples. Raw spectra were post-processed using Compass DataAnalysis 4.2 (Bruker Daltonics, Bremen, Germany) and peaks with a signal-to-noise ratio (S/N) of at least six were exported to mass lists. All exported features were aligned in a matrix containing averaged m/z values (maximum peak alignment window width: ± 1 ppm) and corresponding peak intensities of all analyzed samples. Only m/z features of monoisotopic candidates and those with feasible mass defects were retained in the matrix.

All further data processing was performed using Microsoft Excel 2010 and R Statistical Language (version 3.4.1). Only molecular features detected in at least two of the three replicates (S/N ≥ 6) of one sample group were considered for further data analysis and interpretation. Remaining m/z values were assigned to their unambiguous molecular formulae as already described.

Principal component analysis (PCA), hierarchical cluster analysis (HCA), and analysis of variance (ANOVA) were performed using Perseus 1.5.1.6 (Max Planck Institute of Biochemistry, Germany). For HCA, the Euclidean distance and average linkage were chosen and for ANOVA, a threshold *p-value* of 0.05.

III. Results and discussion

1. Fermentation kinetics and yeast viability

We carried out sequential fermentations to obtain a better understanding of the interaction between *S. cerevisiae* and *L. thermotolerans*. Must was first inoculated with *L. thermotolerans* and 24 h later with *S. cerevisiae* to allow the growth of the non-*Saccharomyces* yeast species before the addition of *S. cerevisiae* (Gobbi et al., 2013; Sadoudi, 2014; Balikci et al., 2016). Sequential fermentations were carried out with or without physical contact to study the consequences of cell-cell interactions. Indeed, such a strategy has been used previously to successfully investigate this type of interaction (Nissen and Arneborg, 2003; Nissen et al., 2003; Renault et al., 2013; Englezos et al., 2019).

1.1. Fermentation kinetics

The kinetics of sugar consumption and ethanol production for each fermentation are presented in fig. 2. Pure fermentation with *S. cerevisiae* (SC) resulted in complete alcoholic fermentation in 10 days, reaching 13.3% (v/v) ethanol with no remaining sugars. Pure fermentation with *L. thermotolerans* (LT) was slower, the percentage of ethanol reaching 12.2% (v/v), but fermentation was not complete, even after 21 days, with remaining sugar at a concentration of approximately 5.7 $g.L^{-1}$. Sequential fermentations with (SF+) or without (SF-) physical contact (fig. 2) were both complete after 16 days, with approximately 13.2% (v/v) ethanol and no remaining sugars. These slower kinetics, relative to those with SC, are a reflection of negative interactions. Thus, yeast viability was monitored to explain this behavior.

1.2. Yeast viability

We used a modified *S. cerevisiae* strain expressing green fluorescent protein (GFP) to separate the *S. cerevisiae* from the non-*Saccharomyces* population, allowing the use of flow cytometry to follow cell viability during pure and sequential fermentations.

Cell viability was determined by PI staining (Delobel et al., 2012) and PI-negative cells were considered to be viable. *L. thermotolerans* cells in LT and both SFs (fig. 3A) showed a maximum viable population of approximately 1.50 x 10^7 $cells.mL^{-1}$ after 24 h of alcoholic fermentation, which remained stable until day 5, with no significant difference between the three conditions (t-test, $p < 0.05$). However, there was a rapid decrease of the viable population in both SFs when the percentage of ethanol reached approximately 10% (v/v), whereas no decrease occurred in LT. This result shows that *S. cerevisiae* had no impact on the growth of *L. thermotolerans* but suggests that *L. thermotolerans* has difficulties in adapting to

294 the faster fermentation kinetics imposed by *S. cerevisiae* in SF, confirming previous results
295 (Nissen et al., 2003; Kapsopoulou et al., 2006; García et al., 2017).

296 We observed the largest viable population (1.42 x 10^8 cells.mL^{-1}) for *S. cerevisiae* cells in SC
297 (fig. 3B), whereas the lowest was found for the two SFs: 6.57 x 10^7 cells.mL^{-1} for SF- and
298 only 9.37 x 10^6 cells.mL^{-1} for SF+, representing a decrease of 54.0 and 93.4% of the viable
299 population, respectively. These results confirm the negative impact of *L. thermotolerans* on *S.*
300 *cerevisiae* in both SFs, with a lower population of *S. cerevisiae*. This decrease was greater in
301 SF+ than SF-, reflecting a cell-cell contact-dependent mechanism, confirming previous
302 reports (Nissen et al., 2003; Renault et al., 2013; Lopez et al., 2014; Rossouw et al., 2018).
303 However, despite the difference in viable populations between the two SFs, the fermentation
304 kinetics were exactly the same (fig. 2). The lower fermentation activity in SF- could be
305 explained by higher competition for nutrients, since a higher biomass was present than in
306 SF+. Nutrient depletion could explain the reduced fermentation activity, as previously
307 described (Bely et al., 1990; Carrau et al., 2008; Barrajón et al., 2011).
308
309 2. Competition for nutrients
310 Yeast under fermentation conditions are subjected to very low concentration of dissolved
311 oxygen, which could affect their growth rate because they require it for unsaturated fatty-acid
312 (UFA) and sterol synthesis, in particular ergosterol, both involved in yeast membrane
313 formation (Salmon et al., 1998; Deytieux et al., 2005). Indeed, under conditions of aerobiosis,
314 yeast are able to synthesize UFA and sterols with a succession of reactions involving oxygen-
315 dependent enzymes (Tehlivets et al., 2007). However, these enzymes are not active in the
316 absence of oxygen. Under such conditions, yeast use fatty acids and sterols present in the
317 medium, *i.e.* fatty acids and phytosterols present in the must in our case. The impact of
318 dissolved oxygen on non-*Saccharomyces*/*S. cerevisiae* interactions is only poorly
319 documented (Hansen et al., 2001; Englezos et al., 2018). These authors showed that the
320 addition of oxygen to co-fermentations of *S. bacillaris* and *S. cerevisiae* promoted the
321 persistence of *S. bacillaris*. Based on these results, the competition for oxygen could, in part,
322 explain the observed interaction. Thus, we monitored the consumption of dissolved oxygen
323 during both SFs and quantified phytosterols in the must before inoculation with *S. cerevisiae*
324 (24 h of fermentation by *L. thermotolerans* alone) to determine whether *L. thermotolerans*
325 consumes these nutrients before *S. cerevisiae* inoculation. We measured dissolved-oxygen
326 levels 3 h (time 0.125 days) after *L. thermotolerans* inoculation and every day thereafter,

before the other analyses, to determine the kinetics of dissolved-oxygen consumption (figure 4). The consumption of dissolved oxygen by *L. thermotolerans* was very rapid, with a drop from 4.1 $mg.L^{-1}$ at T0 to 0.21 $mg.L^{-1}$ after 3 h and down to 0 $mg.L^{-1}$ for all fermentations until day 18, with an increase for SF- by day 21. These results highlight the absence of dissolved oxygen in both SFs. The very low concentration of oxygen present when the fermentation was inoculated with *S. cerevisiae* could explain the lower biomass observed under SF conditions. Indeed, oxygen availability has been shown to affect *S. cerevisiae* biomass production and viability during alcoholic fermentation (Blateyron and Sablayrolles, 2001; Fornairon-Bonnefond and Salmon, 2003). Moreover, it has been recently reported that oxygen availability strongly influences the viability of non-*Saccharomyces* species (Varela et al., 2012; Shekhawat et al., 2017; Englezos et al., 2018). Thus, early consumption of oxygen by *L. thermotolerans* could partially explain the decreased biomass and viability of the yeast during both SFs.

We also monitored phytosterol uptake by *L. thermotolerans* during the first 24 h, before inoculation with *S. cerevisiae*, in parallel to oxygen consumption. The major phytosterol present in the must was β-sitosterol (Table 1), as reported in the literature (Luparia et al., 2004; Rollero et al., 2016), at a concentration of approximately 29 $mg.L^{-1}$, with the two other phytosterols present at lower concentrations, approximately 1.9 $mg.L^{-1}$ for campesterol and 1.6 $mg.L^{-1}$ for stigmasterol. *L. thermotolerans* consumed approximately 68% of the β-sitosterol, 14% of the stigmasterol, and all the campesterol in only 24 h of fermentation. Thus, only a low concentration of the remaining phytosterols were available for *S. cerevisiae* growth under anaerobiosis. Both oxygen and phytosterol uptake by *L. thermotolerans* may explain, in part, the negative observed interaction, which led to a decrease in biomass, viability, and consequently fermentative capacity. Indeed, the stress encountered by *S. cerevisiae* may be explained, in part, by the direct anaerobiosis at the time of inoculation, blocking ergosterol and UFA synthesis, as well as the absence of phytosterols available to replace ergosterol in the membrane, which can affect growth and fermentative activity, as shown by Luparia *et al.* (2004), Deytieux *et al.* (2005) and Salmon, 2006. This is the first time that competition for oxygen and phytosterol has been reported in a yeast-yeast interaction study. Hansen *et al.* (2001) and Englezos *et al.* (2018) previously showed that low oxygen levels affect non-*Saccharomyces* species and phytosterol uptake has only been studied in *S. cerevisiae* strains (Luparia et al., 2004; Rollero et al., 2016).

3. Quantification of YAN and volatile compounds during alcoholic fermentations

3.1. YAN quantification

The nitrogen content of grape must is a key factor for yeast growth and a sufficient quantity is required to avoid stuck/sluggish fermentatio (Wang et al., 2003; Bell and Henschke, 2005; Gobert et al., 2017). An important part of YAN comes from ammonium, which must be in sufficient amounts for the growth of non-*Saccharomyces* and *S. cerevisiae*. Certain amino acids can be used as YAN sources and aromatic amino acids are precursors for volatile compound production, increasing wine complexity (Kemsawasd et al., 2015; González et al., 2018). Thus, we analyzed the consumption of YAN sources during the first day of fermentation by *L. thermotolerans* to assess the remaining YAN sources at the time of *S. cerevisiae* inoculation (Table 2). There was considerable uptake of the various nitrogen sources by *L. thermotolerans*. Among them, Arg, Asn, Gln, Ile, and Ser have been shown to be preferred nitrogen sources for *S. cerevisiae* (Godard et al., 2007; Kemsawasd et al., 2015), meaning that under our conditions, only non-preferential or intermediate sources were available at the time of *S. cerevisiae* inoculation. Thus, consumption of the preferential nitrogen sources by *L. thermotolerans* (> 79%) could explain, in part, the lower biomass and viability of *S. cerevisiae* under both SF conditions than that of pure fermentation, for which all nitrogen sources are available.

Indeed, there must be a synergistic effect between oxygen, phytosterol, and YAN uptake by *L. thermotolerans* that negatively affects the growth of *S. cerevisiae*. It is highly likely that the lower biomass of *S. cerevisiae* under SF conditions is triggered by limited nutrient availability (oxygen, phytosterols, and nitrogen sources).

Aside from the effect on yeast biomass and yeast viability, oxygen, phytosterol, and YAN influence the volatile composition of wine (Hirst and Richter, 2016). Consumption of these nutrients by *L. thermotolerans* could thus affect the volatile composition of wine.

3.2. Volatile-compound quantification

We quantified volatile compounds by HS-SPME-GC/MS for all fermentations to assess the impact of *L. thermotolerans* on SF. This method identified 40 volatile compounds in our fermentations (Table 3). We thus performed PCA analysis based on these 40 volatile compounds. PCA analysis clearly distinguished the three different modalities (fig. 5). Wine produced by SC could be separated from that produced by LT on the basis of higher alcohol content. Wines produced by both yeast species form a distinct group, but there were

observable differences between the SF+ and SF- modalities, which reflect the impact of cell-cell contact on volatile compound production. This is the first time that volatile compounds have been analyzed under SF conditions, with or without cell-cell contact, although several other studies of co-fermentation with *L. thermotolerans* and *S. cerevisiae* have been performed, but not with physical separation, as discussed above.

A detailed examination of volatile compound composition (Table 3) shows that LT resulted in the highest concentration of total alcohols, with approximately 622.7 $mg.L^{-1}$ versus 475.7, 455.2, and 494.3 mg.L-1for SC, SF+, and SF-, respectively. Thus, the presence of *S. cerevisiae* limits the production of higher alcohols by *L. thermotolerans*. These results could reflect a decrease in the viability *L. thermotolerans* after eight days of SF, leading to lower concentrations of higher alcohols than with LT. In contrast, the total concentration of medium-chain fatty acids for LT was approximately 3.6 $mg.L^{-1}$, lower than for SC (12.2 $mg.L^{-1}$). Each SF condition resulted in a specific concentration of these compounds, 7.03 $mg.L^{-1}$ for SF+, representing an intermediate concentration between that of LT and SC, and 14.3 $mg.L^{-1}$for SF- . Our results show that the cell-cell contact modulates the production of medium-chain fatty acids, with an almost two-fold lower concentration for SF+ than SC. Our results contradict those of previous studies, which did not find any differences in medium-chain fatty acid production between co-fermentation of *S. cerevisiae* and *L. thermtolerans* and *S. cerevisiae* pure fermentation (Benito et al., 2015, 2016; Balikci et al., 2016). There were no differences in aldehyde, ketone, or lactone levels between LT, SC, and SF+ but they were slightly lower for SF- than SC and SF+. There were also no significant differences for terpene compounds between conditions. The last compound family that we analyzed was esters. The total concentration of these compounds in LT was 559 $\mu g.L^{-1}$, the lowest for all conditions. Indeed, the total concentration was similar for SC and SF-, 1,725.0 and 1,873.1 $\mu g.L^{-1}$, respectively, whereas SF+ showed an intermediate concentration of 1401.8 $\mu g.L^{-1}$. Globally, the presence of *L. thermotolerans* appears to decrease the concentration of some esters more in SF+ than SF-, which was also observed in the study conducted by Balikci *et al.* (2016) in a 24-h sequential fermentation. These results demonstrate a negative impact of *L. thermotolerans* on *S. cerevisiae* for the production of most esters, showing an effect of cell-cell contact on ester production, whereas these compounds are desirable in wine because of their sweet, floral, or fruity aromas (Beckner Whitener et al., 2015). Studies conducted by Gobbi *et al.* (2013) and Benito *et al.* (2015) on volatile compounds in SF with *L. thermotolerans* and *S. cerevisiae* have shown an increase of ethyl lactate, ethyl hexanoate, and

isoamyl acetate concentrations, with a decrease of those of ethyl octanoate and phenylethyl acetate, as found in our study.

Several studies on nitrogen sources and volatile compounds have attempted to elucidate the relation between amino acids and volatile compounds, two important families for yeast in enological conditions. Indeed, amino-acid precursor and volatile-compound synthesis are linked by regulation of the Ehrlich pathway, which explains the conversion of some amino acids to aromatic volatile compounds (Hazelwood et al., 2008). Thus, the decrease in phenylethyl acetate concentrations, which gives wine a floral aroma, under both conditions of SF can be easily explained by the depletion of phenylalanine by *L. thermotolerans* before inoculation with *S. cerevisiae*. However, recent studies conducted by Crépin *et al.* (2017) and Rollero *et al.* (2017) show that the link between amino acids and volatile compounds is not so simple, even if the influence of YAN on volatile compound production has been confirmed, although it is not fully understood. Their results show that even if phenylalanine is absent for phenylethyl acetate production, the intermediate phenylethyl alcohol is present at the same concentration in all fermentations, meaning that other metabolic pathways may be involved in phenylethyl acetate production. We made a similar observation for isoamyl acetate (banana aroma), which increased under both SF conditions, whereas its precursor, leucine, was also depleted by *L. thermotolerans*.

4. Metabolomic analysis by FT-ICR-MS

We analysed the exo-metabolome at the end of alcoholic fermentation for each fermentation to better understand the nature of the interaction between yeast species, since it has been shown previously that this approach can successfully unravel interaction mechanisms (Liu et al., 2016).

FT-ICR-MS analyses of SC, LT, SF+, and SF- were performed at the end of alcoholic fermentation. We performed a PCA that included all fermentation conditions (fig. 6A). PCA showed that SC, LT, and SF- present different exo-metabolomes, with good separation between SF- *versus* SC, LT, and SF+, according to axis 1 (36.8% of the variability) and a separation between LT *versus* SF-, SC, and SF+, according to axis 2 (20.8% of the variability) (fig. 6A). Based on PCA, SC and SF+ appear to have a more similar exo-metabolome than that of SC *versus* LT or SF-. These results show that a must fermented by a non-*Saccharomyces* yeast, here *L. thermotolerans*, has an exo-metabolome distinct from that of the same must fermented by *S. cerevisiae*. Nevertheless, the association of the two yeast

459 species by physical contact (SF+) shows the dominance of *S. cerevisiae* over *L.*
460 *thermotolerans*, whereas physical separation (SF-) led to the modification of both exo-
461 metabolomes, resulting in a new exo-metabolome different from that of SC or LT. We then
462 analyzed the metabolite composition of each fermentation. A Venn diagram (fig. 6B)
463 highlights the difference in composition between SC, LT, SF+ and SF-. First, there were
464 qualitative differences. For example, only two masses were unique to SC, four to SF+, 28 to
465 SF-, and 24 to LT, whereas 15 masses were unique to SF+ and SC, as well as 91 to SC, SF+
466 and SF-. Each yeast species clearly produced unique metabolites in pure fermentation not
467 found in the others. Moreover, the presence of 28 unique metabolites in SF- show that cell-
468 cell contact modifies the metabolism of *S. cerevisiae* or *L. thermotolerans* as 28 metabolites
469 were unique to SF- and only four to SF+. This diagram also shows that 1,247 masses (66.8%
470 of the total composition) were common to all fermentations, but the concentrations varied,
471 depending on the conditions of fermentation (SC, LT, SF+ and SF-). We performed an
472 ANOVA (threshold *p-value* < 0.05) to find markers that can discriminate between
473 fermentations. Specific markers are represented in a hierarchical cluster analysis (HCA) and
474 in Van Krevelen diagrams, highlighting compound families, coupled to histograms of
475 elemental formula composition (fig 7). HCA (fig. 7A) confirmed the four groups found above
476 by PCA, with a greater distance between LT and the other conditions, as well as a very high
477 similarity between SC and SF+ conditions. Thus, for example, SC markers (fig. 7B, SC) are
478 composed of CHO (blue), CHOS (green), and CHON (orange) in similar quantities (between
479 10 and 15), but CHNOS (red) compounds are present in only low quantities (approximately
480 5). These compounds can be associated mostly with carbohydrate, anthocyanin, and amino-
481 acid families. Each fermentation gave a specific profile in which carbohydrate, amino-acid,
482 nucleic-acid, and anthocyanin families were found in all (fig. 7B). However, the intensity of
483 the compounds in each family differed greatly, depending on the fermentation condition,
484 showing that each yeast species has a different metabolism. This metabolism is modified
485 when both yeast species are put together, with a different response, depending on whether the
486 cells are physically separated or not. Moreover, the quantity of compounds was greater for LT
487 and SF-, with approximately 170 for LT (mostly CHO and CHON compounds) and 320 for
488 SF- (mostly CHO and CHON compounds), than for SC (approximately 50) and SF+
489 (approximately 105), meaning that a higher diversity of compounds was found in LT and SF-.
490 Each yeast clearly has its own impact on SF+ and SF- in terms of chemical composition and
491 these results show that interactions between a non-*Saccharomyces* yeast and *S. cerevisiae*

affect not only the volatile compound profile but also the metabolite profile, with specific exo-metabolomes for SC, LT, SF+, and SF- fermentations.

We carried the analysis further by making pairwise comparisons for all conditions, *i.e.* LT/SC, LT/SF+, SC/SF+, LT/SF-, and SC/SF-, to highlight markers for each pair (fig. 8). First, PCAs were performed for each pair to assess the separation of each fermentation according to axis 1, representing 86.2% of the variability for LT/SC, 89.7% for LT/SF-, 61.6% for SF+/SF-, 46.9% for LT/SF+, and 38.1% for SC/SF+, again highlighting the difference between LT and both SF conditions, as well as the similarity between the SC and SF+ conditions (fig. 8, left). Second, we used ANOVA (threshold *p-value* < 0.05), to find markers for each pair of conditions, represented in H/C *vs.* O/C van Krevelen diagrams coupled to histograms of elemental formula composition (fig. 8, middle and right). Carbohydrate, amino-acid, nucleic-acid, and anthocyanin families were mostly represented in all comparisons. The next step consisted of annotating these biomarkers and correlating them with the metabolic pathways involved. We sought biomarkers in several databases (KEGG, Lipidmap, YMDB, Metlin and an in-house plant and wine database) and generated a Search and color KEGG visualization (supp. fig. 2) (Kanehisa and Goto, 2000; Kanehisa et al., 2012). Based on the 76 identified metabolic pathways, most LT and SF- biomarkers are involved in carbohydrate, carbon fixation, and amino-acid metabolism. We were unable to identify any biomarkers for SC and only two for SF+, which are involved in carbohydrate and nucleotide metabolism (supp. fig. 2). This highlights the complex metabolite composition of wine, which is still poorly understood, as reported previously by studies using FT-ICR-MS on wine (Roullier-Gall et al., 2014a, 2014b; Roullier-Gall et al., 2015).

These results show that metabolites produced by yeast under our different conditions result mainly from sugar and nitrogen source metabolism (also shown in supp. fig. 3), which represents 20 of the 76 identified metabolic pathways. This is not surprising because of the lack of these nutrients at the end of alcoholic fermentation.

These results provide new insights for the further study of interactions between non-*Saccharomyces* and *S. cerevisiae* by comparing specific exo-metabolomes (composed of specific markers) of each fermentation, which may reflect the impact of interactions on metabolite production.

Thus, the biomarkers found in our fermentations may be useful given the high intensity of metabolites specific for fermentations performed with *L. thermotolerans*, *S. cerevisiae*, and SF of both species, with or without cell-cell contact.

5. Conclusion

Here, we aimed to investigate the interactions that occur between *S. cerevisiae* and *L. thermotolerans* during alcoholic fermentation of grape must. The results obtained from all analyses performed in this study highlight a negative interaction between the two species to the detriment of *S. cerevisiae*, due to a cell-cell contact mechanism (SF+ fermentation) and the consumption of essential nutrients by *L. thermotolerans* during both SF conditions. However, *L. thermotolerans* was also negatively affected by the presence of *S. cerevisiae* under both SF conditions, even if the quantification of volatile compounds showed that *L. thermotolerans* is able to modulate aroma complexity without differences between the two SF conditions. Moreover, this study provides, a comparison of the exo-metabolomes of *L. thermotolerans* and *S. cerevisiae* pure fermentations, as well as SF with both species, with or without cell-cell contact. This comparison showed that interactions also affect metabolite production by *L. thermotolerans* and *S. cerevisiae* during alcoholic fermentation in a different manner as a function of the condition.

In conclusion, this study provides new insights concerning the interaction of *L. thermotolerans* and *S. cerevisiae* during the alcoholic fermentation of grape must. However, further study of the cell-cell contact mechanism and further identification of the metabolites needs to be carried out to better understand the interactions between these two yeast species and to investigate if these interactions between the two species are strain dependent.

6. Acknowledgments

We thank the other members of the VAlMiS laboratory for their assistance, in particular Antoine Gobert for amino-acid quantification and the other PhD students for their help and advice.

7. Funding

This work was supported by the Ministère de l'Enseignement Supérieur, de la Recherche et de l'Innovation and the Fond Européen De Développement Régional (FEDER) through the PO FEDER-FSE Bourgogne 2014/2020 programs.

8. References

Albergaria, H., Francisco, D., Gori, K., Arneborg, N., Gírio, F., 2009. Saccharomyces cerevisiae CCMI 885 secretes peptides that inhibit the growth of some non-Saccharomyces wine-related strains. Appl. Microbiol. Biotechnol. 86, 965–972. https://doi.org/10.1007/s00253-009-2409-6

Alexandre, H., Charpentier, C., 1998. Biochemical aspects of stuck and sluggish fermentation in grape must. J. Ind. Microbiol. Biotechnol. 20, 20–27.

Balikci, E.K., Tanguler, H., Jolly, N.P., Erten, H., 2016. Influence of Lachancea thermotolerans on cv. Emir wine fermentation. Yeast 33, 313–321. https://doi.org/10.1002/yea.3166

Barbosa, C., Mendes-Faia, A., Lage, P., Mira, N.P., Mendes-Ferreira, A., 2015. Genomic expression program of Saccharomyces cerevisiae along a mixed-culture wine fermentation with Hanseniaspora guilliermondii. Microb. Cell Factories 14. https://doi.org/10.1186/s12934-015-0318-1

Barrajón, N., Arévalo-Villena, M., Úbeda, J., Briones, A., 2011. Enological properties in wild and commercial Saccharomyces cerevisiae yeasts: relationship with competition during alcoholic fermentation. World J. Microbiol. Biotechnol. 27, 2703–2710. https://doi.org/10.1007/s11274-011-0744-0

Beckner Whitener, M.E., Carlin, S., Jacobson, D., Weighill, D., Divol, B., Conterno, L., Du Toit, M., Vrhovsek, U., 2015. Early fermentation volatile metabolite profile of non-Saccharomyces yeasts in red and white grape must: A targeted approach. LWT - Food Sci. Technol. 64, 412–422. https://doi.org/10.1016/j.lwt.2015.05.018

Bell, S.-J., Henschke, P.A., 2005. Implications of nitrogen nutrition for grapes, fermentation and wine. Aust. J. Grape Wine Res. 11, 242–295.

Bely, M., Sablayrolles, J.-M., Barre, P., 1990. Automatic detection of assimilable nitrogen deficiencies during alcoholic fermentation in oenological conditions. J. Ferment. Bioeng. 70, 246–252. https://doi.org/10.1016/0922-338X(90)90057-4

Benito, Á., Calderón, F., Palomero, F., Benito, S., 2016. Quality and Composition of Airén Wines Fermented by Sequential Inoculation of Lachancea thermotolerans and Saccharomyces cerevisiae. Food Technol. Biotechnol. 54, 135–144. https://doi.org/10.17113/ftb.54.02.16.4220

Benito, S., 2018. The impact of <Emphasis Type="Italic">Torulaspora delbrueckii</Emphasis> yeast in winemaking. Appl. Microbiol. Biotechnol. 1–14. https://doi.org/10.1007/s00253-018-8849-0

Benito, S., Hofmann, T., Laier, M., Lochbühler, B., Schüttler, A., Ebert, K., Fritsch, S., Röcker, J., Rauhut, D., 2015. Effect on quality and composition of Riesling wines fermented by sequential inoculation with non-<Emphasis Type="Italic">Saccharomyces</Emphasis> and <Emphasis Type="Italic">Saccharomyces cerevisiae</Emphasis>. Eur. Food Res. Technol. 241, 707–717. https://doi.org/10.1007/s00217-015-2497-8

Blateyron, L., Sablayrolles, J.M., 2001. Stuck and Slow Fermentations in Enology: Statistical Study of Causes and Effectiveness of Combined Additions of Oxygen and Diammonium Phosphate 6.

Branco, P., Francisco, D., Chambon, C., Hébraud, M., Arneborg, N., Almeida, M.G., Caldeira, J., Albergaria, H., 2014. Identification of novel GAPDH-derived antimicrobial peptides secreted by Saccharomyces cerevisiae and involved in wine microbial interactions. Appl. Microbiol. Biotechnol. 98, 843–853. https://doi.org/10.1007/s00253-013-5411-y

Carrau, F.M., Medina, K., Farina, L., Boido, E., Henschke, P.A., Dellacassa, E., 2008. Production of fermentation aroma compounds by *Saccharomyces cerevisiae* wine yeasts: effects of yeast assimilable nitrogen on two model strains. FEMS Yeast Res. 8, 1196–1207. https://doi.org/10.1111/j.1567-1364.2008.00412.x

Ciani, M., 1997. Role, enological properties and potential biotechnological use of non-Saccharomyces wine yeasts [WWW Document]. URL https://www.researchgate.net/profile/Maurizio_Ciani/publication/284677825_Role_enological_properties_and_potential_use_of_non-Saccharomyces_wine_yeasts/links/565eb5b908ae1ef92983e4b3.pdf (accessed 8.22.16).

Ciani, M., Capece, A., Comitini, F., Canonico, L., Siesto, G., Romano, P., 2016. Yeast Interactions in Inoculated Wine Fermentation. Front. Microbiol. 7. https://doi.org/10.3389/fmicb.2016.00555

Crépin, L., Truong, N.M., Bloem, A., Sanchez, I., Dequin, S., Camarasa, C., 2017. Management of multiple nitrogen sources during wine fermentation by S. cerevisiae. Appl Env. Microbiol AEM.02617-16. https://doi.org/10.1128/AEM.02617-16

Delobel, P., Pradal, M., Blondin, B., Tesniere, C., 2012. A 'fragile cell' sub-population revealed during cytometric assessment of Saccharomyces cerevisiae viability in lipid-limited alcoholic fermentation. Lett. Appl. Microbiol. 55, 338–344. https://doi.org/10.1111/j.1472-765X.2012.03301.x

Deytieux, C., Mussard, L., Biron, M.-J., Salmon, J.-M., 2005. Fine measurement of ergosterol requirements for growth of Saccharomyces cerevisiae during alcoholic fermentation. Appl. Microbiol. Biotechnol. 68, 266–271. https://doi.org/10.1007/s00253-004-1872-3

Englezos, V., Cravero, F., Torchio, F., Rantsiou, K., Ortiz-Julien, A., Lambri, M., Gerbi, V., Rolle, L., Cocolin, L., 2018. Oxygen availability and strain combination modulate yeast growth dynamics in mixed culture fermentations of grape must with Starmerella bacillaris and Saccharomyces cerevisiae. Food Microbiol. 69, 179–188. https://doi.org/10.1016/j.fm.2017.08.007

Englezos, V., Rantsiou, K., Giacosa, S., Río Segade, S., Rolle, L., Cocolin, L., 2019. Cell-to-cell contact mechanism modulates Starmerella bacillaris death in mixed culture fermentations with Saccharomyces cerevisiae. Int. J. Food Microbiol. 289, 106–114. https://doi.org/10.1016/j.ijfoodmicro.2018.09.009

Esteve-Zarzoso, B., Manzanares, P., Ramon, D., Querol, A., 1998. The role of non-Saccharomyces yeasts in industrial winemaking. Int. Microbiol. 1, 143–148.

Fleet, G.H., 2008. Wine yeasts for the future. FEMS Yeast Res. 8, 979–995. https://doi.org/10.1111/j.1567-1364.2008.00427.x

Fornairon-Bonnefond, C., Salmon, J.-M., 2003. Impact of Oxygen Consumption by Yeast Lees on the Autolysis Phenomenon during Simulation of Wine Aging on Lees. J. Agric. Food Chem. 51, 2584–2590. https://doi.org/10.1021/jf0259819

García, M., Esteve-Zarzoso, B., Arroyo, T., 2016. Non-Saccharomyces Yeasts: Biotechnological Role for Wine Production, in: Morata, A., Loira, I. (Eds.), Grape and Wine Biotechnology. InTech. https://doi.org/10.5772/64957

García, M., Esteve-Zarzoso, B., Crespo, J., Cabellos, J.M., Arroyo, T., 2017. Yeast Monitoring of Wine Mixed or Sequential Fermentation Made by Native Strains from D.O. "Vinos de Madrid" Using Real Time Quantitative PCR. Front. Microbiol. 8. https://doi.org/10.3389/fmicb.2017.02520

Gobbi, M., Comitini, F., Domizio, P., Romani, C., Lencioni, L., Mannazzu, I., Ciani, M., 2013. Lachancea thermotolerans and Saccharomyces cerevisiae in simultaneous and sequential co-fermentation: A strategy to enhance acidity and improve the overall

quality of wine. Food Microbiol. 33, 271–281. https://doi.org/10.1016/j.fm.2012.10.004
Gobert, A., Tourdot-Maréchal, R., Morge, C., Sparrow, C., Liu, Y., Quintanilla-Casas, B., Vichi, S., Alexandre, H., 2017. Non-Saccharomyces Yeasts Nitrogen Source Preferences: Impact on Sequential Fermentation and Wine Volatile Compounds Profile. Front. Microbiol. 8. https://doi.org/10.3389/fmicb.2017.02175
Godard, P., Urrestarazu, A., Vissers, S., Kontos, K., Bontempi, G., Helden, J. van, André, B., 2007. Effect of 21 Different Nitrogen Sources on Global Gene Expression in the Yeast Saccharomyces cerevisiae. Mol. Cell. Biol. 27, 3065–3086. https://doi.org/10.1128/MCB.01084-06
González, B., Vázquez, J., Morcillo-Parra, M.Á., Mas, A., Torija, M.J., Beltran, G., 2018. The production of aromatic alcohols in non-Saccharomyces wine yeast is modulated by nutrient availability. Food Microbiol. 74, 64–74. https://doi.org/10.1016/j.fm.2018.03.003
Hansen, E.H., Nissen, P., Sommer, P., Nielsen, J.C., Arneborg, N., 2001. The effect of oxygen on the survival of non-Saccharomyces yeasts during mixed culture fermentations of grape juice with Saccharomyces cerevisiae. J. Appl. Microbiol. 91, 541–547. https://doi.org/10.1046/j.1365-2672.2001.01426.x
Hazelwood, L.A., Daran, J.-M., Maris, A.J.A. van, Pronk, J.T., Dickinson, J.R., 2008. The Ehrlich Pathway for Fusel Alcohol Production: a Century of Research on Saccharomyces cerevisiae Metabolism. Appl Env. Microbiol 74, 2259–2266. https://doi.org/10.1128/AEM.02625-07
Hirst, M.B., Richter, C.L., 2016. Review of Aroma Formation through Metabolic Pathways of Saccharomyces cerevisiae in Beverage Fermentations. Am. J. Enol. Vitic. 67, 361–370. https://doi.org/10.5344/ajev.2016.15098
Jolly, J., Augustyn, O.P.H., Pretorius, I.S., others, 2006. The role and use of non-Saccharomyces yeasts in wine production. South Afr. J. Enol. Vitic. 27, 15.
Jolly, N.P., Varela, C., Pretorius, I.S., 2014. Not your ordinary yeast: non-Saccharomyces yeasts in wine production uncovered. FEMS Yeast Res. 14, 215–237. https://doi.org/10.1111/1567-1364.12111
Kanehisa, M., Goto, S., 2000. KEGG: Kyoto Encyclopedia of Genes and Genomes. Nucleic Acids Res. 28, 27–30. https://doi.org/10.1093/nar/28.1.27
Kanehisa, M., Goto, S., Sato, Y., Furumichi, M., Tanabe, M., 2012. KEGG for integration and interpretation of large-scale molecular data sets. Nucleic Acids Res. 40, D109–D114. https://doi.org/10.1093/nar/gkr988
Kapsopoulou, K., Kapaklis, A., Spyropoulos, H., 2005. Growth and Fermentation Characteristics of a Strain of the Wine Yeast Kluyveromyces thermotolerans Isolated in Greece. World J. Microbiol. Biotechnol. 21, 1599–1602. https://doi.org/10.1007/s11274-005-8220-3
Kapsopoulou, K., Mourtzini, A., Anthoulas, M., Nerantzis, E., 2006. Biological acidification during grape must fermentation using mixed cultures of Kluyveromyces thermotolerans and Saccharomyces cerevisiae. World J. Microbiol. Biotechnol. 23, 735–739. https://doi.org/10.1007/s11274-006-9283-5
Kemsawasd, V., Viana, T., Ardö, Y., Arneborg, N., 2015. Influence of nitrogen sources on growth and fermentation performance of different wine yeast species during alcoholic fermentation. Appl. Microbiol. Biotechnol. 99, 10191–10207. https://doi.org/10.1007/s00253-015-6835-3
Liu, Y., Forcisi, S., Harir, M., Deleris-Bou, M., Krieger-Weber, S., Lucio, M., Longin, C., Degueurce, C., Gougeon, R.D., Schmitt-Kopplin, P., Alexandre, H., 2016. New molecular evidence of wine yeast-bacteria interaction unraveled by non-targeted

703 exometabolomic profiling. Metabolomics 12, 1–16. https://doi.org/10.1007/s11306-
704 016-1001-1
705 Liu, Y., Rousseaux, S., Tourdot-Maréchal, R., Sadoudi, M., Gougeon, R., Schmitt-Kopplin,
706 P., Alexandre, H., 2015. Wine microbiome, a dynamic world of microbial interactions.
707 Crit. Rev. Food Sci. Nutr. 0, 00–00. https://doi.org/10.1080/10408398.2014.983591
708 Longin, C., Petitgonnet, C., Guilloux-Benatier, M., Rousseaux, S., Alexandre, H., 2017.
709 Application of flow cytometry to wine microorganisms. Food Microbiol. 62, 221–231.
710 https://doi.org/10.1016/j.fm.2016.10.023
711 Lopez, C.L.F., Beaufort, S., Brandam, C., Taillandier, P., 2014. Interactions between
712 Kluyveromyces marxianus and Saccharomyces cerevisiae in tequila must type
713 medium fermentation. World J. Microbiol. Biotechnol. 30, 2223–2229.
714 https://doi.org/10.1007/s11274-014-1643-y
715 Luparia, V., Soubeyrand, V., Berges, T., Julien, A., Salmon, J.-M., 2004. Assimilation of
716 grape phytosterols by Saccharomyces cerevisiae and their impact on enological
717 fermentations. Appl. Microbiol. Biotechnol. 65, 25–32.
718 https://doi.org/10.1007/s00253-003-1549-3
719 Marsit, S., Mena, A., Bigey, F., Sauvage, F.-X., Couloux, A., Guy, J., Legras, J.-L., Barrio,
720 E., Dequin, S., Galeote, V., 2015. Evolutionary Advantage Conferred by an
721 Eukaryote-to-Eukaryote Gene Transfer Event in Wine Yeasts. Mol. Biol. Evol. 32,
722 1695–1707. https://doi.org/10.1093/molbev/msv057
723 Mora, J., Barbas, J.I., Mulet, A., 1990. Growth of yeast species during the fermentation of
724 musts inoculated with Kluyveromyces thermotolerans and Saccharomyces cerevisiae.
725 Am. J. Enol. Vitic. 41, 156–159.
726 Nissen, P., Arneborg, N., 2003. Characterization of early deaths of non- Saccharomyces
727 yeasts in mixed cultures with Saccharomyces cerevisiae. Arch. Microbiol. 180, 257–
728 263. https://doi.org/10.1007/s00203-003-0585-9
729 Nissen, P., Nielsen, D., Arneborg, N., 2003. Viable Saccharomyces cerevisiae cells at high
730 concentrations cause early growth arrest of non-Saccharomyces yeasts in mixed
731 cultures by a cell–cell contact-mediated mechanism. Yeast 20, 331–341.
732 https://doi.org/10.1002/yea.965
733 Renault, P.E., Albertin, W., Bely, M., 2013. An innovative tool reveals interaction
734 mechanisms among yeast populations under oenological conditions. Appl. Microbiol.
735 Biotechnol. 97, 4105–4119. https://doi.org/10.1007/s00253-012-4660-5
736 Rojas, V., Gil, J.V., Piñaga, F., Manzanares, P., 2001. Studies on acetate ester production by
737 non-Saccharomyces wine yeasts. Int. J. Food Microbiol. 70, 283–289.
738 https://doi.org/10.1016/S0168-1605(01)00552-9
739 Rollero, S., Mouret, J.-R., Bloem, A., Sanchez, I., Ortiz□Julien, A., Sablayrolles, J.-M.,
740 Dequin, S., Camarasa, C., 2017. Quantitative 13C-isotope labelling-based analysis to
741 elucidate the influence of environmental parameters on the production of fermentative
742 aromas during wine fermentation. Microb. Biotechnol. 10, 1649–1662.
743 https://doi.org/10.1111/1751-7915.12749
744 Rollero, S., Mouret, J.-R., Sanchez, I., Camarasa, C., Ortiz-Julien, A., Sablayrolles, J.-M.,
745 Dequin, S., 2016. Key role of lipid management in nitrogen and aroma metabolism in
746 an evolved wine yeast strain. Microb. Cell Factories 15.
747 https://doi.org/10.1186/s12934-016-0434-6
748 Romano, P., Suzzi, G., Comi, G., Zironi, R., 1992. Higher alcohol and acetic acid production
749 by apiculate wine yeasts. J. Appl. Bacteriol. 73, 126–130.
750 https://doi.org/10.1111/j.1365-2672.1992.tb01698.x

751 Rossouw, D., Meiring, S.P., Bauer, F.F., 2018. Modifying Saccharomyces cerevisiae
752 Adhesion Properties Regulates Yeast Ecosystem Dynamics. mSphere 3, e00383-18.
753 https://doi.org/10.1128/mSphere.00383-18
754 Roullier-Gall, Chloé, Boutegrabet, L., Gougeon, R.D., Schmitt-Kopplin, P., 2014a. A grape
755 and wine chemodiversity comparison of different appellations in Burgundy: Vintage
756 vs terroir effects. Food Chem. 152, 100–107.
757 https://doi.org/10.1016/j.foodchem.2013.11.056
758 Roullier-Gall, Chloé, Witting, M., Gougeon, R.D., Schmitt-Kopplin, P., 2014b. High
759 precision mass measurements for wine metabolomics. Front. Chem. 2.
760 https://doi.org/10.3389/fchem.2014.00102
761 Roullier-Gall, C., Witting, M., Tziotis, D., Ruf, A., Gougeon, R.D., Schmitt-Kopplin, P.,
762 2015. Integrating analytical resolutions in non-targeted wine metabolomics.
763 Tetrahedron 71, 2983–2990. https://doi.org/10.1016/j.tet.2015.02.054
764 Sablayrolles, J.-M., Dubois, C., Manginot, C., Roustan, J.-L., Barre, P., 1996. Effectiveness of
765 combined ammoniacal nitrogen and oxygen additions for completion of sluggish and
766 stuck wine fermentations. J. Ferment. Bioeng. 82, 377–381.
767 https://doi.org/10.1016/0922-338X(96)89154-9
768 Sadoudi, M., 2014. Intérêts biotechnologiques des levures indigènes non saccharomyces
769 [WWW Document]. http://www.theses.fr. URL http://www.theses.fr/s81726 (accessed
770 9.28.15).
771 Sadoudi, M., Tourdot-Maréchal, R., Rousseaux, S., Steyer, D., Gallardo-Chacón, J.-J.,
772 Ballester, J., Vichi, S., Guérin-Schneider, R., Caixach, J., Alexandre, H., 2012. Yeast–
773 yeast interactions revealed by aromatic profile analysis of Sauvignon Blanc wine
774 fermented by single or co-culture of non-Saccharomyces and Saccharomyces yeasts.
775 Food Microbiol. 32, 243–253. https://doi.org/10.1016/j.fm.2012.06.006
776 Salmon, J.-M., 2006. Interactions between yeast, oxygen and polyphenols during alcoholic
777 fermentations: Practical implications. LWT - Food Sci. Technol., European
778 Symposium on Apple Processing 39, 959–965.
779 https://doi.org/10.1016/j.lwt.2005.11.005
780 Salmon, J.-M., Fornairon, C., Barre, P., 1998. Determination of oxygen utilization pathways
781 in an industrial strain of Saccharomyces cerevisiae during enological fermentation. J.
782 Ferment. Bioeng. 86, 154–163. https://doi.org/10.1016/S0922-338X(98)80054-8
783 Shekhawat, K., Bauer, F.F., Setati, M.E., 2017. Impact of oxygenation on the performance of
784 three non-Saccharomyces yeasts in co-fermentation with Saccharomyces cerevisiae.
785 Appl. Microbiol. Biotechnol. 101, 2479–2491. https://doi.org/10.1007/s00253-016-
786 8001-y
787 Strauss, M. l. a., Jolly, N. p., Lambrechts, M. g., Van Rensburg, P., 2001. Screening for the
788 production of extracellular hydrolytic enzymes by non-Saccharomyces wine yeasts. J.
789 Appl. Microbiol. 91, 182–190. https://doi.org/10.1046/j.1365-2672.2001.01379.x
790 Taillandier, P., Ramon Portugal, F., Fuster, A., Strehaiano, P., 2007. Effect of ammonium
791 concentration on alcoholic fermentation kinetics by wine yeasts for high sugar content.
792 Food Microbiol. 24, 95–100. https://doi.org/10.1016/j.fm.2006.04.002
793 Tehlivets, O., Scheuringer, K., Kohlwein, S.D., 2007. Fatty acid synthesis and elongation in
794 yeast. Biochim. Biophys. Acta BBA - Mol. Cell Biol. Lipids, Regulation of Lipid
795 Metabolism in Yeast 1771, 255–270. https://doi.org/10.1016/j.bbalip.2006.07.004
796 Torija, M.J., Rozès, N., Poblet, M., Guillamón, J.M., Mas, A., 2001. Yeast population
797 dynamics in spontaneous fermentations: Comparison between two different wine-
798 producing areas over a period of three years. Antonie Van Leeuwenhoek 79, 345–352.
799 https://doi.org/10.1023/A:1012027718701

Valera, M.J., Morcillo-Parra, M.Á., Zagórska, I., Mas, A., Beltran, G., Torija, M.J., 2019. Effects of melatonin and tryptophol addition on fermentations carried out by Saccharomyces cerevisiae and non-Saccharomyces yeast species under different nitrogen conditions. Int. J. Food Microbiol. 289, 174–181. https://doi.org/10.1016/j.ijfoodmicro.2018.09.013

Varela, C., Torrea, D., Schmidt, S.A., Ancin-Azpilicueta, C., Henschke, P.A., 2012. Effect of oxygen and lipid supplementation on the volatile composition of chemically defined medium and Chardonnay wine fermented with Saccharomyces cerevisiae. Food Chem. 135, 2863–2871. https://doi.org/10.1016/j.foodchem.2012.06.127

Wang, C., Mas, A., Esteve-Zarzoso, B., 2016. The Interaction between Saccharomyces cerevisiae and Non-Saccharomyces Yeast during Alcoholic Fermentation is Species and Strain Specific. Food Microbiol. 7, 502. https://doi.org/10.3389/fmicb.2016.00502

Wang, X.D., Bohlscheid, J.C., Edwards, C.G., 2003. Fermentative activity and production of volatile compounds by Saccharomyces grown in synthetic grape juice media deficient in assimilable nitrogen and/or pantothenic acid. J. Appl. Microbiol. 94, 349–359.

Zhang, B., Luan, Y., Duan, C., Yan, G., 2018. Use of Torulaspora delbrueckii co-fermentation with two Saccharomyces cerevisiae strains with different aromatic characteristic to improve the diversity of red wine aroma profile. Front. Microbiol. 9. https://doi.org/10.3389/fmicb.2018.00606

Zupan, J., Avbelj, M., Butinar, B., Kosel, J., Šergan, M., Raspor, P., 2013. Monitoring of Quorum-Sensing Molecules during Minifermentation Studies in Wine Yeast. J. Agric. Food Chem. 61, 2496–2505. https://doi.org/10.1021/jf3051363

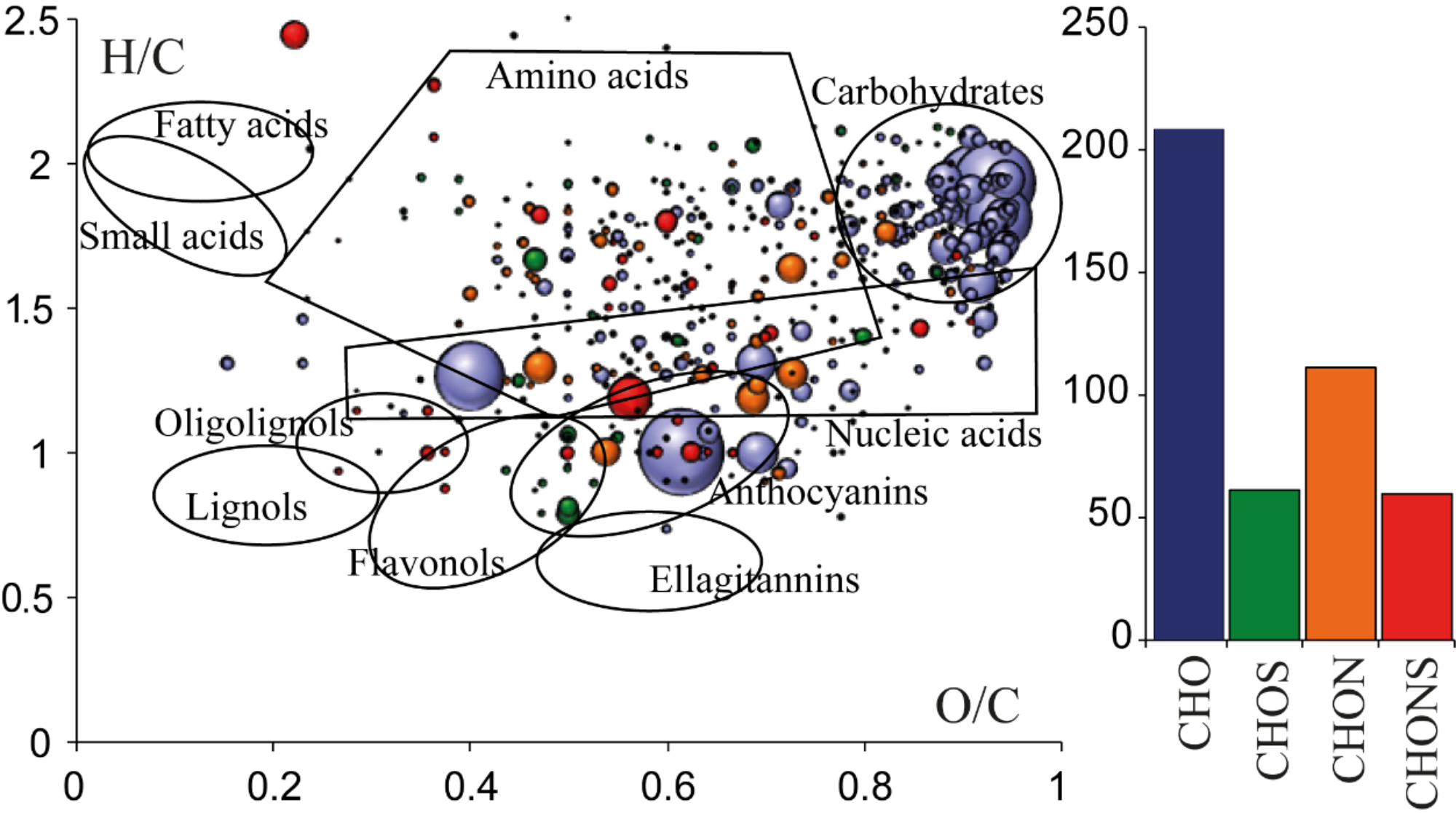
H/C
O/C
Amino acids
Carbohydrates
Fatty acids
Small acids
Oligolignols
Lignols
Flavonols
Ellagitannins
Anthocyanins
Nucleic acids
2.5
2
1.5
1
0.5
0
0
0.2
0.4
0.6
0.8
1
250
200
150
100
50
0
CHO
CHOS
CHON
CHONS

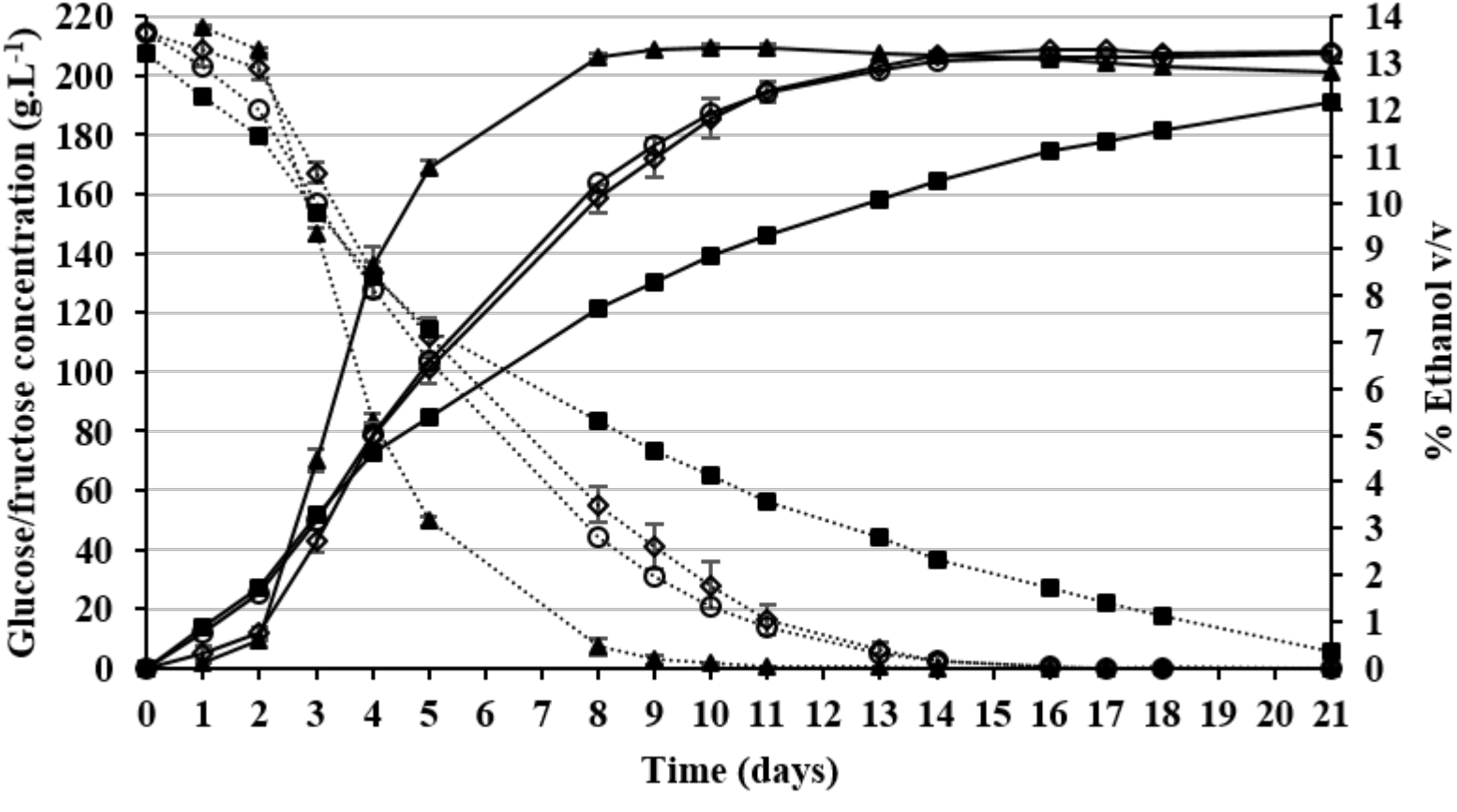
Glucose/fructose concentration (g.L-1)
% Ethanol v/v
Time (days)
0
20
40
60
80
100
120
140
160
180
200
220
0
1
2
3
4
5
6
7
8
9
10
11
12
13
14
0 1 2 3 4 5 6 7 8 9 10 11 12 13 14 15 16 17 18 19 20 21

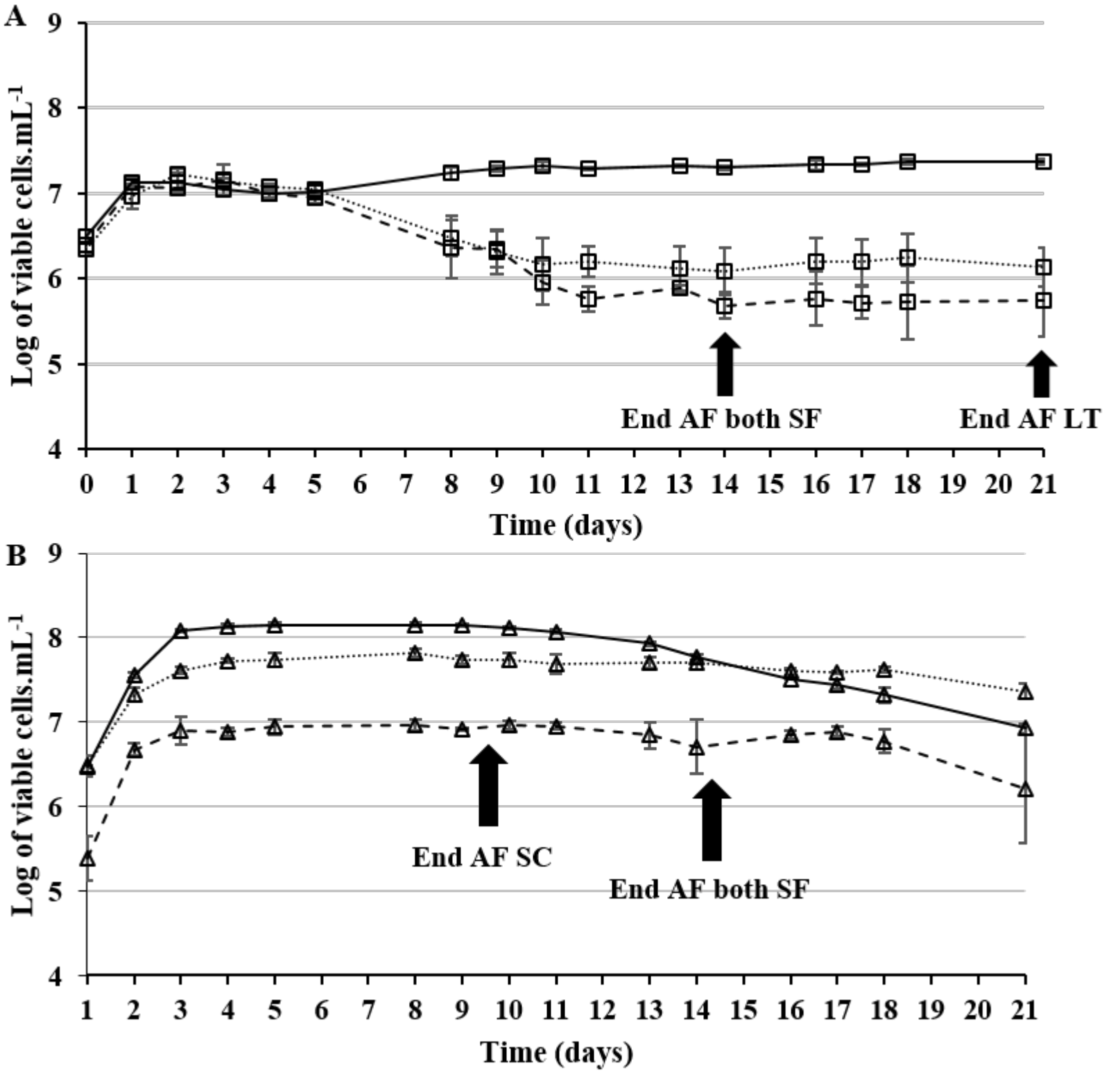
A
Log of viable cells.mL-1
9
8
7
6
5
4
End AF both SF
End AF LT
0 1 2 3 4 5 6 7 8 9 10 11 12 13 14 15 16 17 18 19 20 21
Time (days)
B
Log of viable cells.mL-1
9
8
7
6
5
4
End AF SC
End AF both SF
1 2 3 4 5 6 7 8 9 10 11 12 13 14 15 16 17 18 19 20 21
Time (days)

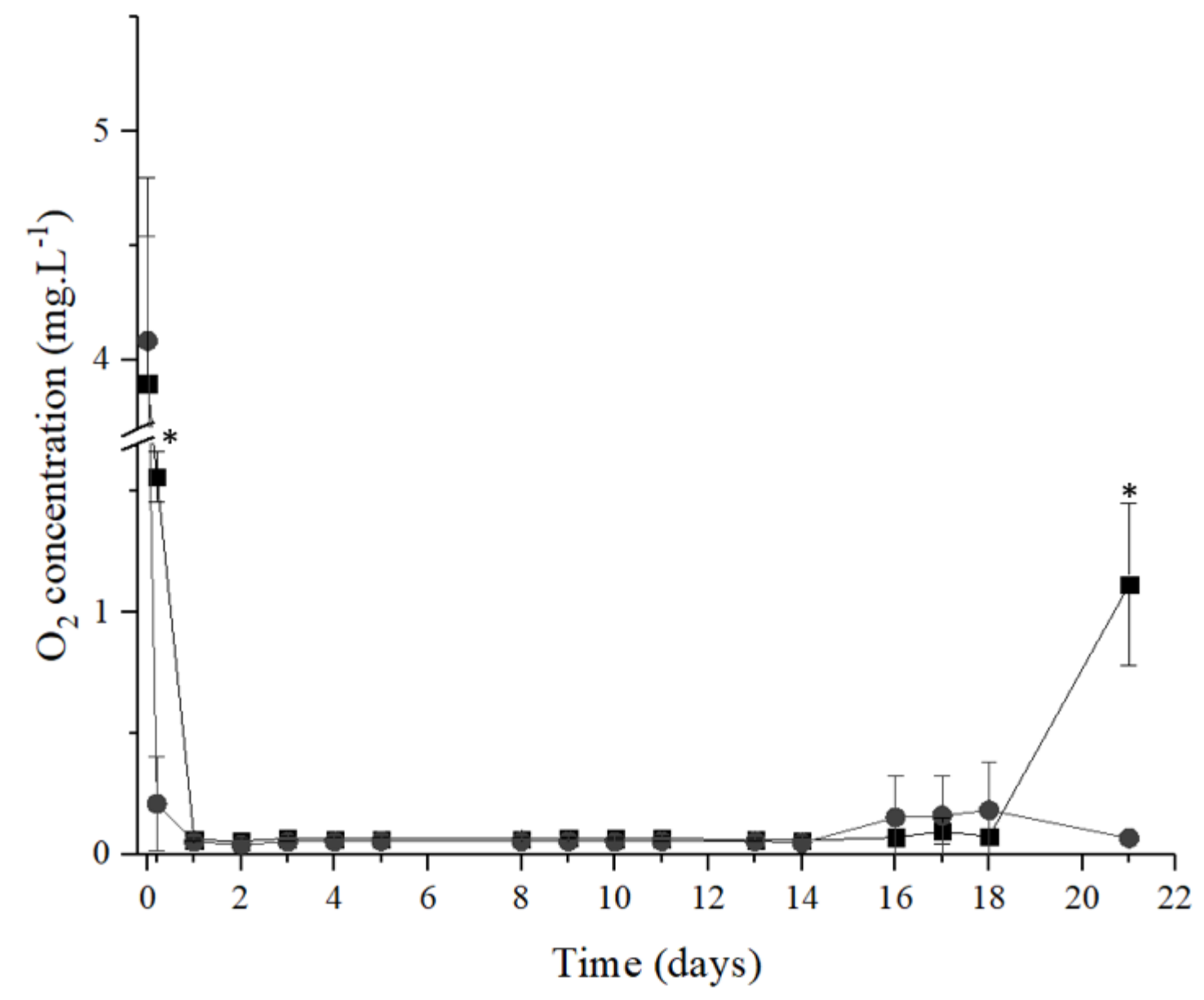
5
4
1
0
O_2 concentration (mg.L^{-1})
*
*
0
2
4
6
8
10
12
14
16
18
20
22
Time (days)

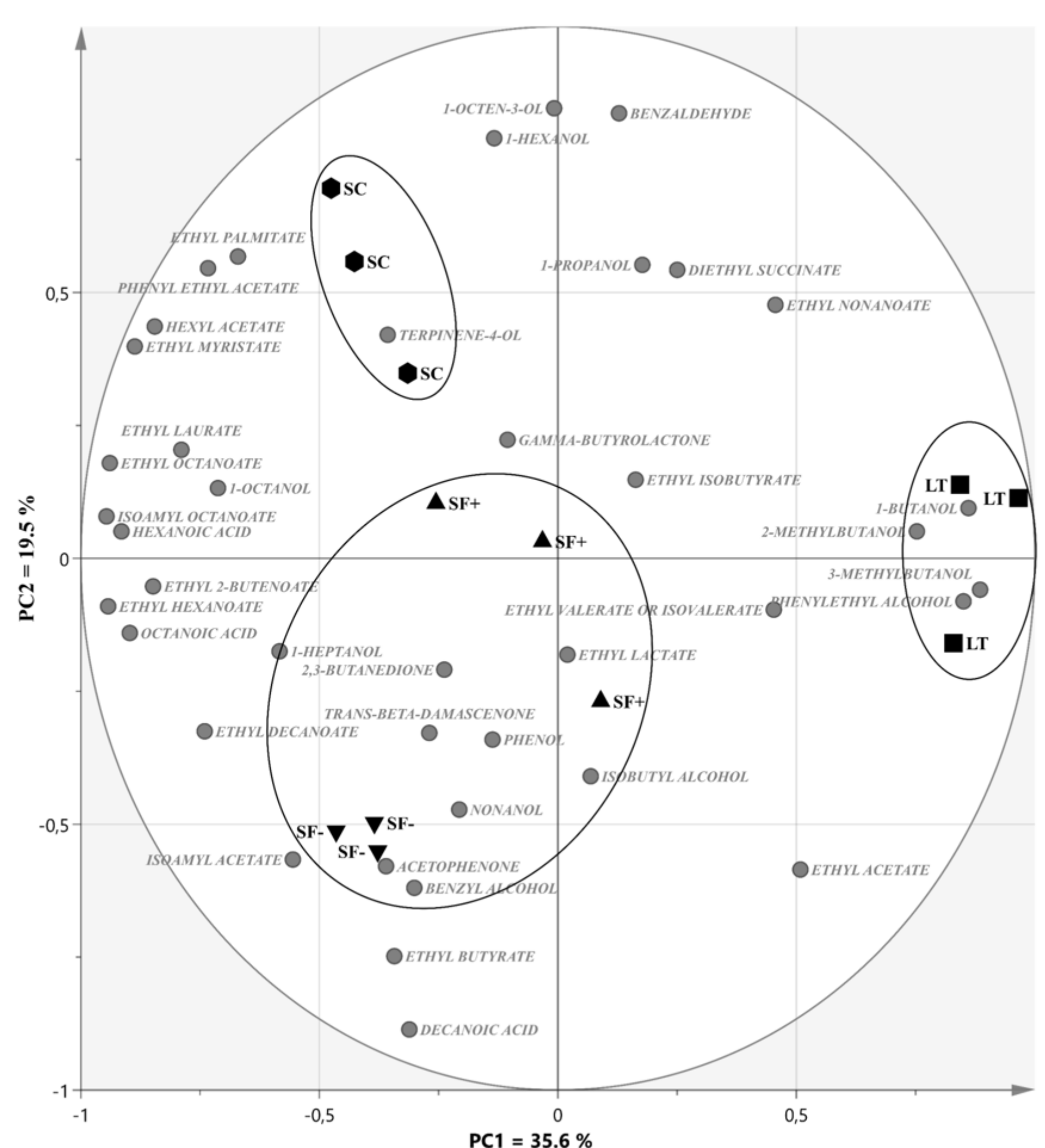
1-OCTEN-3-OL
BENZALDEHYDE
1-HEXANOL
SC
SC
SC
ETHYL PALMITATE
PHENYL ETHYL ACETATE
1-PROPANOL
DIETHYL SUCCINATE
ETHYL NONANOATE
HEXYL ACETATE
ETHYL MYRISTATE
TERPINENE-4-OL
ETHYL LAURATE
ETHYL OCTANOATE
1-OCTANOL
ISOAMYL OCTANOATE
HEXANOIC ACID
GAMMA-BUTYROLACTONE
ETHYL ISOBUTYRATE
SF+
SF+
LT
LT
LT
1-BUTANOL
2-METHYLBUTANOL
3-METHYLBUTANOL
PHENYLETHYL ALCOHOL
ETHYL 2-BUTENOATE
ETHYL HEXANOATE
OCTANOIC ACID
ETHYL VALERATE OR ISOVALERATE
1-HEPTANOL
2,3-BUTANEDIONE
ETHYL LACTATE
SF+
TRANS-BETA-DAMASCENONE
ETHYL DECANOATE
PHENOL
ISOBUTYL ALCOHOL
NONANOL
SF-
SF-
SF-
ISOAMYL ACETATE
ACETOPHENONE
ETHYL ACETATE
BENZYL ALCOHOL
ETHYL BUTYRATE
DECANOIC ACID
0,5
0
-0,5
-1
-1
-0,5
0
0,5
PC2 = 19.5 %
PC1 = 35.6 %

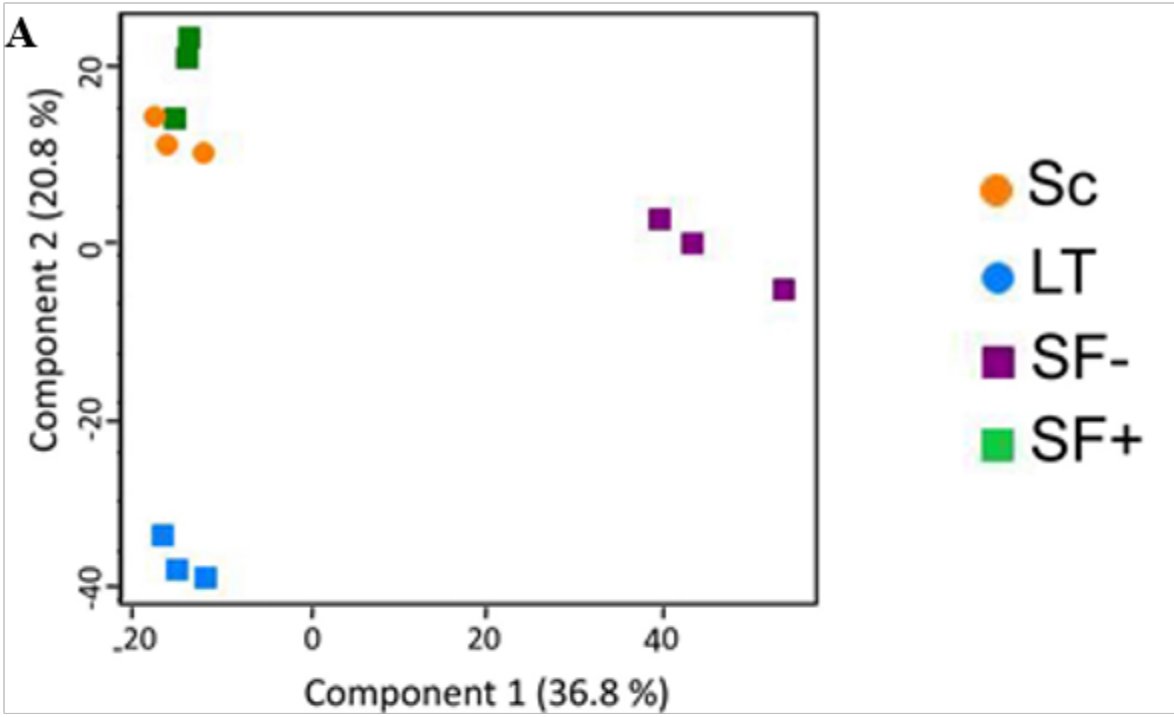
A
Component 2 (20.8 %)
20
0
-20
-40
-20
0
20
40
Component 1 (36.8 %)
Sc
LT
SF-
SF+

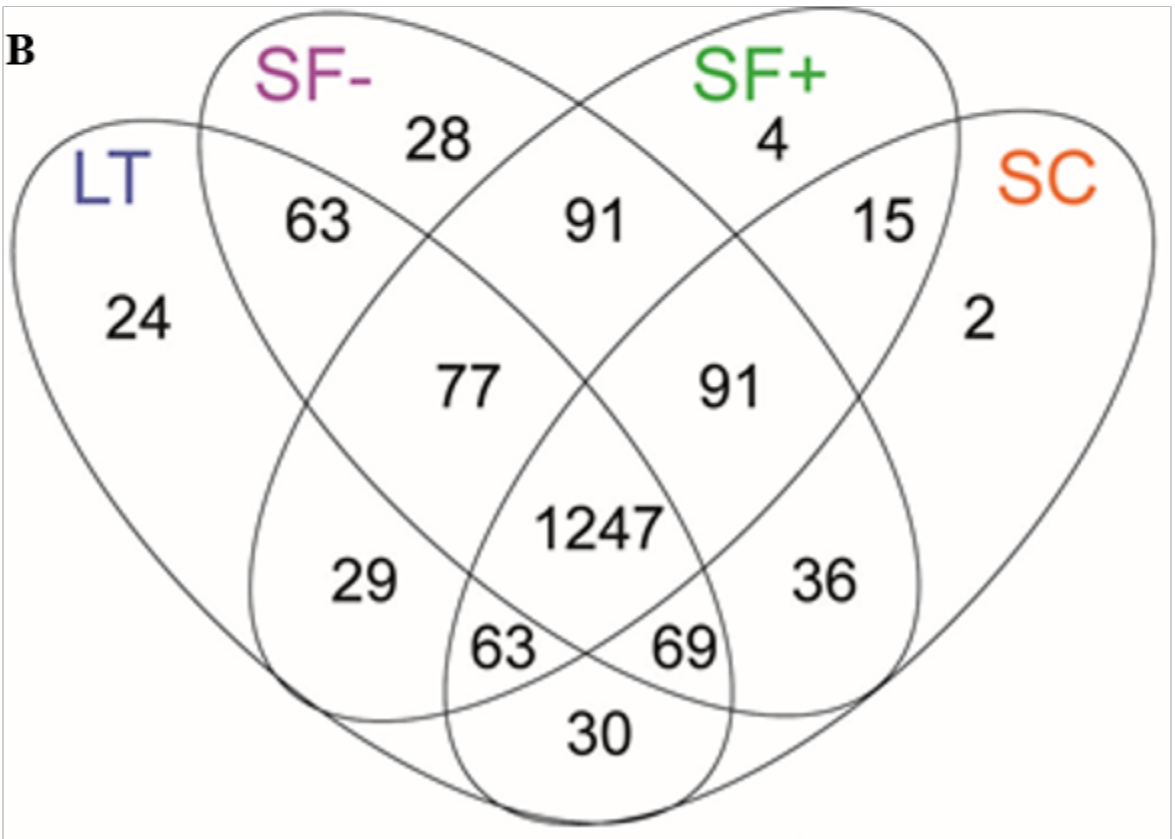
B
SF-
SF+
LT
SC
28
4
63
91
15
24
2
77
91
1247
29
36
63
69
30

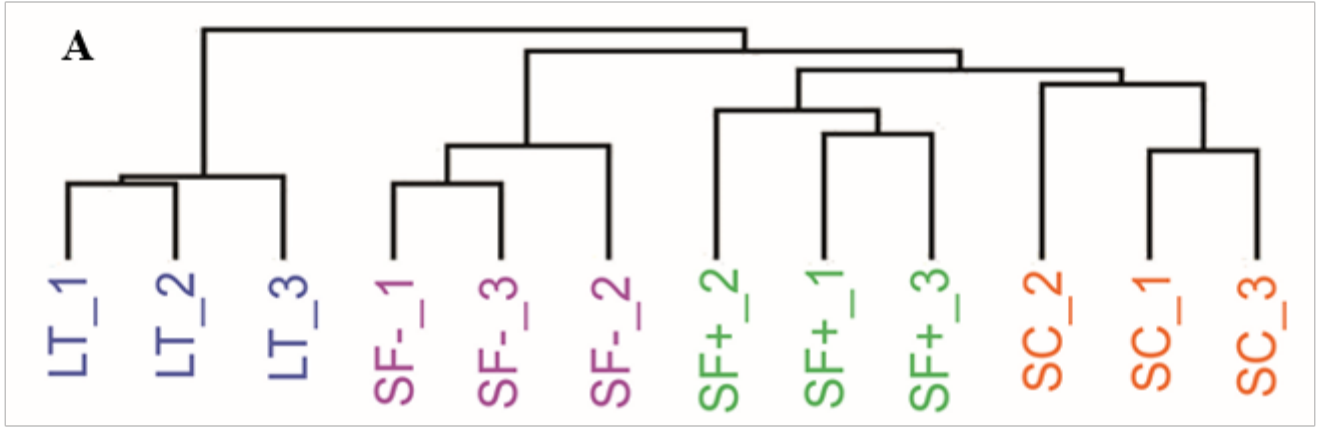
A
LT_1
LT_2
LT_3
SF-_1
SF-_3
SF-_2
SF+_2
SF+_1
SF+_3
SC_2
SC_1
SC_3

B

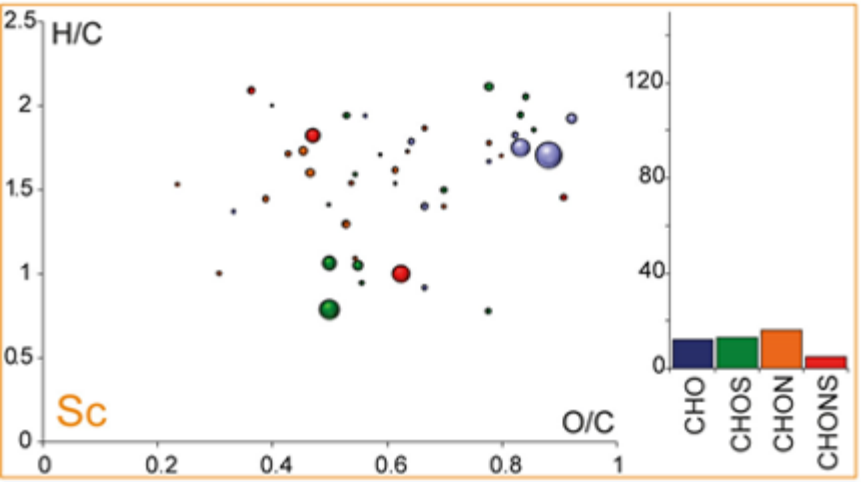
H/C
O/C
Sc
CHO
CHOS
CHON
CHONS

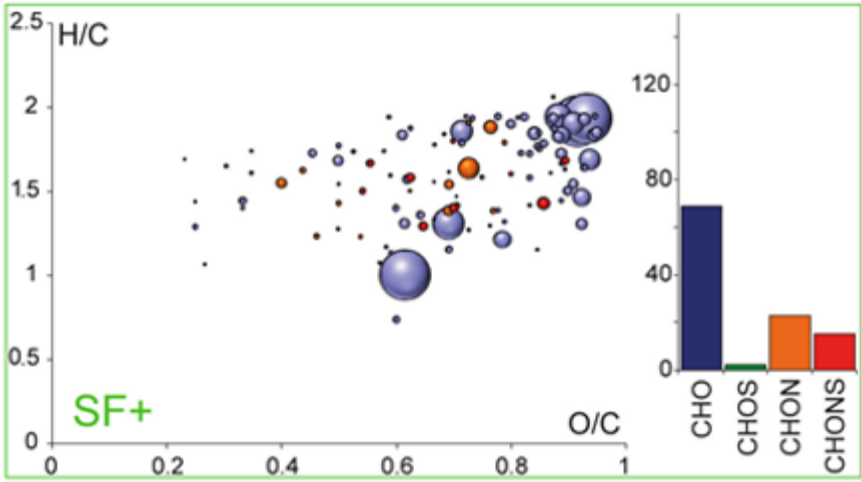
H/C
O/C
SF+
CHO
CHOS
CHON
CHONS

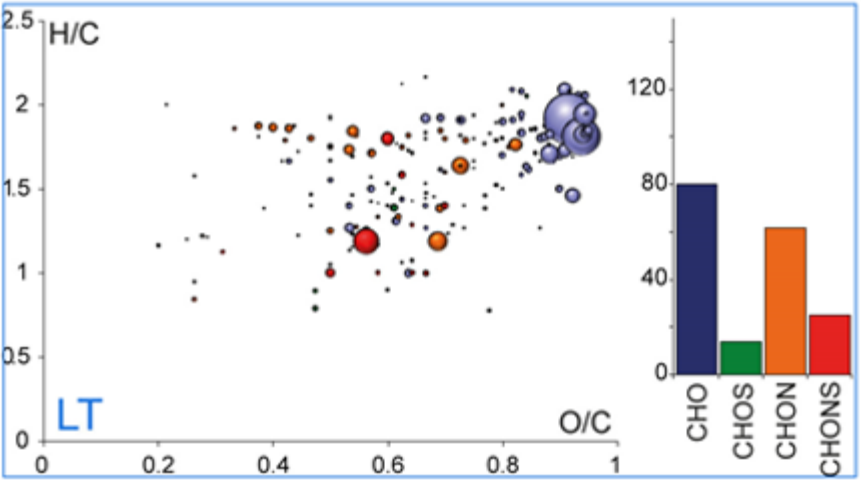
H/C
O/C
LT
CHO
CHOS
CHON
CHONS

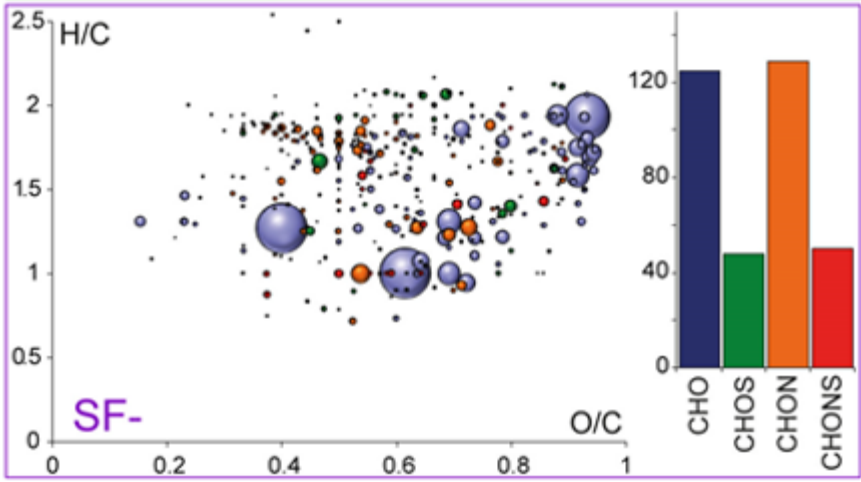
H/C
O/C
SF-
CHO
CHOS
CHON
CHONS

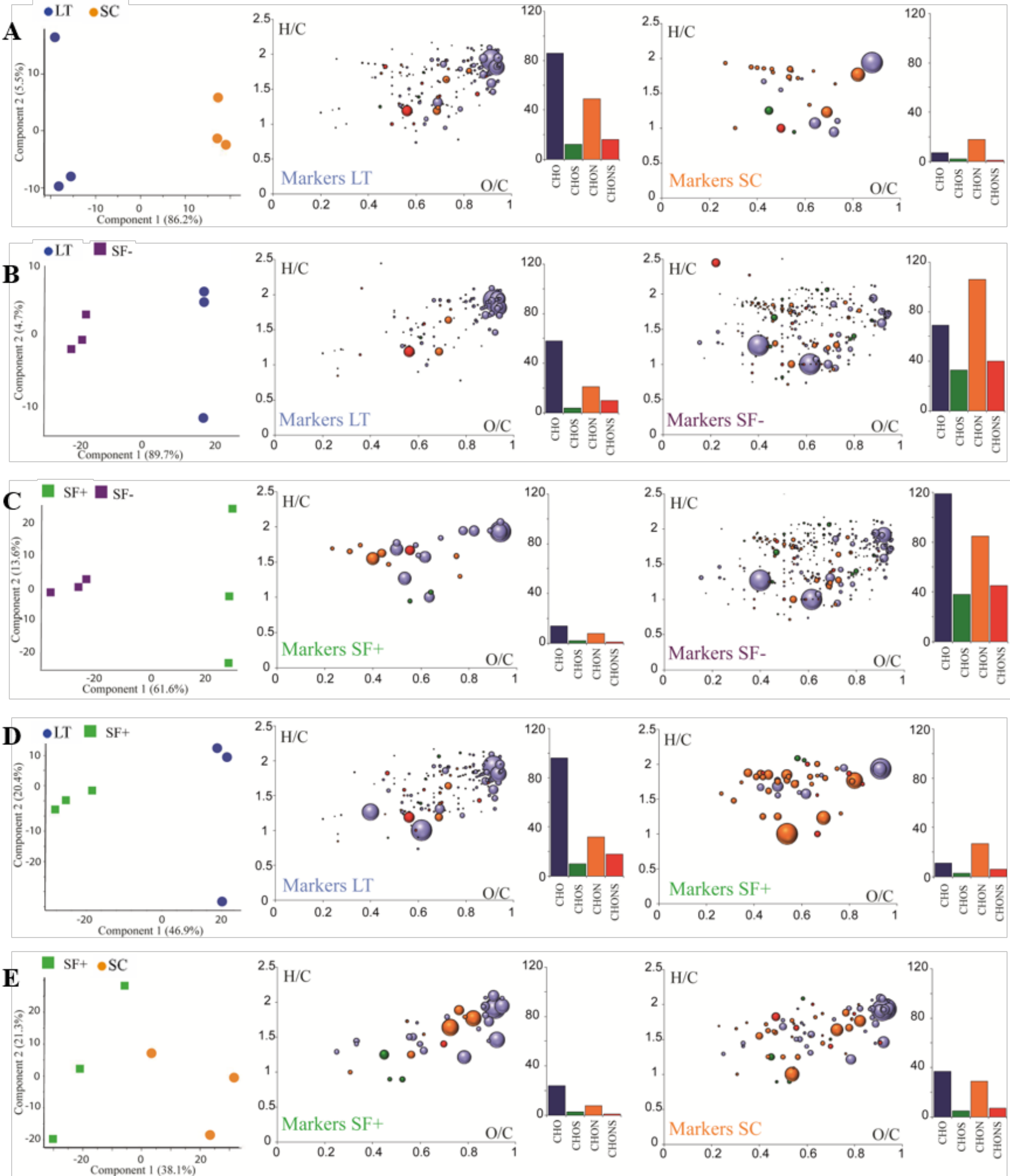
A
LT
SC
Component 2 (5.5%)
Component 1 (86.2%)
H/C
O/C
Markers LT
Markers SC
CHO
CHOS
CHON
CHONS
B
LT
SF-
Component 2 (4.7%)
Component 1 (89.7%)
Markers LT
Markers SF-
C
SF+
SF-
Component 2 (13.6%)
Component 1 (61.6%)
Markers SF+
Markers SF-
D
LT
SF+
Component 2 (20.4%)
Component 1 (46.9%)
Markers LT
Markers SF+
E
SF+
SC
Component 2 (21.3%)
Component 1 (38.1%)
Markers SF+
Markers SC

Figure 1: (Left) H/C vs. O/C van Krevelen diagram of common masses found in all fermentations (LT, SC, SF+ and SF-) with the region where metabolite families are represented and (right) histograms representing the abundance of metabolites composed with CHO, CHOS, CHON or CHONS atoms.

Figure 2: Fermentation kinetics with sugar consumptions (glucose and fructose) and ethanol production by yeasts in pure and sequential fermentations with and without dialysis membrane in white must at 20°C: ··▲·· Glucose/fructose and -▲- % Ethanol v/v *S. cerevisiae* pure fermentation (SC); ··■·· Glucose/fructose and -■- % Ethanol v/v *L. thermotolerans* pure fermentation (LT); ··♦·· Glucose/Fructose and -♦- % Ethanol v/v sequential fermentation without contact (SF-);··○·· Glucose/fructose and -○- % Ethanol v/v sequential fermentation with contact (SF+). Error bars represent the standard deviation of the results.

Figure 3: Curves representing the concentration of PI negative cells (viable cells, log representation) in pure and sequential fermentations in white must at 20°C:
(A) □ *L. thermotolerans* pure fermentation (LT); − − □ − − *L. thermotolerans* SF+; ··□·· *L. thermotolerans* SF-.
(B) ▲ *S. cerevisiae* pure fermentation (SC); − − ▲− − *S. cerevisiae* SF+; ··▲·· *S. cerevisiae* SF-.
Error bars represent the standard deviation of the results.

Figure 4: Consumption of dissolve oxygen during alcoholic fermentation of both sequential fermentations with (SF+) or without (SF-) contact: -●- SF+; -■- SF-.
* significative difference (T-test. *p-value* < 0.05) between both fermentations and error bars represent the standard deviation of the results.

Figure 5: Biplot of the principal component analysis (PC1 vs. PC2) for volatile compounds found in each fermentations. Ellipses represent clusters obtained from HCA.
SF+: sequential fermentation with contact
SF-: sequential fermentation without contact (both compartments)
SC: *S. cerevisiae* pure fermentation
LT: *L. thermotolerans* pure fermentation
Figure 6: (A) Principal component analysis (PC1 vs. PC2) of metabolite profiles for each fermentation condition. (B) Venn diagram representing metabolites found exclusively in each fermentation as well as those found in two or more fermentations, with 1247 metabolites that are common to all fermentations.

Figure 7: (A) Hierarchical cluster analysis (HCA) obtained after ANOVA (threshold *p-value* < 0.05). (B) H/C vs. O/C Van Krevelen diagrams representing masses from the 1247 common masses with a higher intensity in SC, LT, SF+ or SF- after ANOVA (*p-value* < 0.05) with histograms representing their composition and number of elemental formula (CHO, CHOS, CHON or CHONS compounds). Bubble sizes indicate relative intensities of corresponding peaks in the spectra.

Figure 8: (A, B, C, D and E, left) Principal component analysis (PC1 *vs.* PC2) of both fermentations for each couple of conditions and (A, B, C, D and E, middle and right) H/C *vs.* O/C Van Krevelen diagrams representing specific metabolites found in both fermentations of each couple described as

markers coupled to histograms of elemental formula composition. Bubble sizes indicate relative intensities of corresponding peaks in the spectra.

Table 1: Concentration of phytosterols ($mg.L^{-1}$) in the must and after 24 h of alcoholic fermentation by *L. thermotolerans* before *S. cerevisiae* inoculation.
nd, non determined.

	Sterol concentration ($mg.L^{-1}$)		
	Must (T0)	**T24 h before *S. cerevisiae* inoculation**	**% of decrease**
ergosterol	nd	nd	nd
campesterol	1.9 ± 0.1	nd	nd
stigmasterol	1.6 ± 0.3	1.4 ± 0.04	14.0 ± 12.0
β-sitosterol	28.8 ± 1.2	9.2 ± 1.4	68.0 ± 3.8

Table 2: Concentration of amino acids and ammonium (mg of $N.L^{-1}$) in the must and after the first 24 hours of fermentation with *L. thermotolerans* in LT, as well as the percentage of decrease representing the consumption of each compound.
* Indicates aromatic amino acids.

	Concentration (mg $N.L^{-1}$)		
YAN	Must (T0)	T24h	% of decrease
Alanine	22.78 ± 0.44	11.36 ± 3.18	50.2 ± 5.0
Arginine	315.03 ± 2.38	39.08 ± 34.28	87.6 ± 1.5
Asparagine	2.70 ± 0.12	0.05 ± 0.40	98.2 ± 3.2
Aspartic acid	3.99 ± 0.12	0.54 ± 0.52	86.4 ± 0.6
Cysteine	0.47 ± 0.41	0.02 ± 0.19	87.3 ± 18.3
GABA	4.53 ± 0.09	4.41 ± 0.18	2.6 ± 6.8
Glutamic acid	5.71 ± 0.12	1.93 ± 0.94	66.2 ± 3.4
Glutamine	41.35 ± 0.89	3.44 ± 4.01	91.7 ± 1.1
Glycine	1.96 ± 0.11	0.90 ± 0.13	54.0 ± 8.4
Histidine*	13.52 ± 0.37	0.01 ± 1.75	99.9 ± 0.2
Isoleucine	1.62 ± 0.14	0.11 ± 0.25	93.0 ± 3.4
Leucine	2.33 ± 0.03	0.16 ± 0.17	92.9 ± 7.0
Lysine	0.04 ± 0.07	0.04 ± 0.22	/
Methionine	0.96 ± 0.24	0.21 ± 0.12	75.4 ± 20.6
NH4+	242 ± 2	163 ± 18	32.6 ± 9.1
Phenylalanine*	10.15 ± 0.06	0.03 ± 0.92	99.7 ± 0.2
Proline	83.86 ± 1.33	83.66 ± 7.13	0.11 ± 13.0
Serine	19.23 ± 0.24	2.76 ± 2.51	85.7 ± 2.7
Threonine	15.81 ± 0.65	0.80 ± 1.55	94.9 ± 1.1
Tyrosine*	3.87 ± 0.01	0.57 ± 0.43	85.2 ± 3.3
Valine	3.83 ± 0.08	0.80 ± 0.44	79.2 ± 3.1

Table 3: Concentration of volatile compounds at the end of AF for each fermentation (SC, LT, SF+ and SF-). Values with the same letters a, b, c or d were not significantly different in Tukey's test (95%); nd stands for non determined. Aroma descriptors inspired by Beckner Whitener et al. (2015).

Volatile compounds (µg.L^{-1})	Aroma descriptors	LT	SC	SF+	SF-
Alcohols					
1-PROPANOL	weak fusel	2636.9 ± 609.1^{a}	2619.5 ± 552.5^{a}	2938.3 ± 680.9^{a}	1989.4 ± 600.6^{a}
ISOBUTYL ALCOHOL		14957.5 ± 1546.9^{a}	13593.4 ± 3444.2^{a}	16923.5 ± 2000.3^{a}	15962.0 ± 2956.7^{a}
1-BUTANOL		1595.1 ± 588.0^{a}	407.4 ± 357.1^{b}	287.4 ± 173.0^{b}	422.8 ± 216.6^{b}
3-METHYLBUTANOL		64147.9 ± 10420.4^{a}	36481.7 ± 8337.5^{b}	37475.9 ± 6178.1^{b}	41503.1 ± 5689.8^{b}
2-METHYLBUTANOL		351686.0 ± 27545.4^{a}	289206.6 ± 41799.3^{b}	272122.5 ± 27895.6^{b}	295422.7 ± 30539.1^{b}
1-HEXANOL	green	3555.6 ± 633.8^{ab}	4412.8 ± 499.4^{a}	4119.5 ± 1006.1^{a}	2932.8 ± 461.5^{b}
1-OCTEN-3-OL	mushroom	46.0 ± 10.4^{ab}	56.6 ± 12.7^{a}	41.7 ± 11.6^{ab}	35.0 ± 10.7^{b}
1-HEPTANOL	leafy	146.6 ± 35.3^{b}	493.5 ± 58.6^{a}	555.9 ± 284.4^{a}	592.9 ± 278.2^{a}
1-OCTANOL	waxy	109.0 ± 26.8^{b}	244.4 ± 15.4^{a}	99.3 ± 20.4^{b}	228.9 ± 43.5^{a}
NONANOL	fruity	227.2 ± 43.6^{a}	217.5 ± 46.4^{a}	304.1 ± 61.7^{a}	295.7 ± 88.0^{a}
BENZYL ALCOHOL	fruity	1.0 ± 1.0^{b}	0.9 ± 0.6^{b}	1.0 ± 1.1^{b}	7.2 ± 5.9^{a}
PHENYLETHYL ALCOHOL	rose	183182.9 ± 18256.1^{a}	127596.2 ± 9981.1^{b}	119724.4 ± 17352.4^{b}	134448.6 ± 8110.8^{b}
PHENOL		395.9 ± 134.2^{a}	384.8 ± 220.5^{a}	589.1 ± 257.1^{a}	486.4 ± 97.6^{a}
Total		622687.6 ± 41831.0^{a}	475715.5 ± 54330.3^{b}	455182.5 ± 48966.9^{b}	494327.2 ± 24460.0^{b}
Medium chain fatty acids					
HEXANOIC ACID	sour	1050.2 ± 93.1^{c}	4051.7 ± 217.7^{a}	2109.2 ± 300.2^{b}	3938.8 ± 406.4^{a}
OCTANOIC ACID	rancid	1739.9 ± 188.8^{d}	7605.2 ± 824.2^{b}	3984.0 ± 335.5^{c}	8679.0 ± 573.7^{a}
DECANOIC ACID	unpleasant	785.1 ± 116.9^{b}	531.2 ± 73.4^{c}	941.0 ± 142.3^{b}	1651.6 ± 207.4^{a}
Total		3575.1 ± 367.3^{d}	12188.2 ± 965.3^{b}	7034.2 ± 719.8^{c}	14269.4 ± 896.3^{a}
Aldehydes, ketones and lactones					
BENZALDEHYDE	almond	4012.7 ± 376.1^{a}	4469.8 ± 362.2^{a}	4396.9 ± 635.7^{a}	2850.2 ± 889.8^{b}
ACETOPHENONE	almond, sweet, floral	103.6 ± 12.5^{b}	89.0 ± 13.2^{b}	249.1 ± 67.6^{ab}	332.1 ± 188.7^{a}
2,3-BUTANEDIONE		529.8 ± 326.4^{a}	608.1 ± 232.7^{a}	568.9 ± 296.6^{a}	723.1 ± 247.9^{a}
GAMMA-BUTYROLACTONE		0.3 ± 0.05^{a}	0.3 ± 0.09^{a}	0.3 ± 0.05^{a}	0.3 ± 0.07^{a}
Total		4646.4 ± 415.5^{ab}	5167.3 ± 529.1^{a}	5215.3 ± 639.4^{a}	3905.6 ± 456.4^{b}
Terpenes					
TERPINENE-4-OL	spicy, mentol	0.7 ± 0.5^{a}	5.3 ± 6.5^{a}	0.5 ± 0.2^{a}	2.3 ± 2.6^{a}
TRANS-BETA-DAMASCENONE	rose	0.5 ± 0.3^{a}	0.5 ± 0.1^{a}	0.6 ± 0.2^{a}	0.6 ± 0.2^{a}
Total		1.2 ± 0.6^{a}	5.8 ± 6.5^{a}	1.0 ± 0.3^{a}	2.8 ± 2.2^{a}
Esters					
ETHYL ACETATE	fruity or ascescent	102.5 ± 14.3^{a}	35.9 ± 8.3^{b}	102.0 ± 10.3^{a}	91.1 ± 18.1^{a}
ETHYL ISOBUTYRATE		2.0 ± 0.5^{a}	1.7 ± 1.0^{a}	2.3 ± 1.0^{a}	1.7 ± 0.7^{a}
ETHYL BUTYRATE	fruity	1.5 ± 1.0^{b}	1.3 ± 0.2^{b}	1.6 ± 0.5^{ab}	2.5 ± 0.7^{a}
ETHYL VALERATE OR ISOVALERATE	fruity	0.2 ± 0.03^{a}	0.2 ± 0.04^{ab}	0.2 ± 0.04^{b}	0.20 ± 0.04^{ab}
ISOAMYL ACETATE	banana	19.0 ± 3.0^{b}	23.7 ± 2.7^{b}	52.5 ± 21.8^{a}	65.2 ± 8.8a
ETHYL 2-BUTENOATE		nd^{b}	0.2 ± 0.1^{a}	0.1 ± 0.08^{a}	0.2 ± 0.1^{a}
ETHYL HEXANOATE	fruity	324.6 ± 50.3^{c}	996.4 ± 78.0^{a}	719.6 ± 84.1^{b}	1126.0 ± 134.4^{a}
HEXYL ACETATE	banana	1.7 ± 0.2^{c}	26.9 ± 3.1^{a}	13.8 ± 10.5^{b}	16.2 ± 2.3^{b}
ETHYL LACTATE		46.6 ± 7.2^{b}	nd^{b}	194.9 ± 57.1^{a}	46.4 ± 15.1^{b}
ETHYL OCTANOATE	apricot	45.5 ± 8.4^{d}	576.8 ± 58.2^{a}	272.6 ± 40.4^{c}	479.5 ± 89.3^{b}
ETHYL NONANOATE		4.0 ± 0.5^{a}	3.5 ± 0.4^{ab}	3.6 ± 1.0^{ab}	2.8 ± 0.6^{b}
ETHYL DECANOATE	sweet	5.2 ± 0.4^{c}	12.5 ± 1.2^{b}	20.9 ± 3.5^{a}	18.6 ± 1.6^{a}
ISOAMYL OCTANOATE	sweet	0.2 ± 0.05^{c}	0.6 ± 0.1^{a}	0.3 ± 0.06^{b}	0.6 ± 0.05^{a}
DIETHYL SUCCINATE	fruity	0.8 ± 0.6^{a}	0.8 ± 0.3^{a}	0.8 ± 0.2^{a}	0.6 ± 0.1^{a}
PHENYL ETHYL ACETATE	floral	2.1 ± 0.2^{d}	34.2 ± 1.7^{a}	8.0 ± 3.4^{c}	15.1 ± 1.5^{b}
ETHYL LAURATE		0.8 ± 0.3^{b}	1.4 ± 0.4^{a}	1.4 ± 0.3^{a}	1.2 ± 0.3^{ab}
ETHYL MYRISTATE		1.3 ± 0.4^{c}	5.3 ± 0.7^{a}	4.0 ± 1.1^{b}	3.6 ± 0.9^{b}
ETHYL PALMITATE		1.1 ± 0.2^{c}	3.7 ± 1.0^{a}	3.3 ± 1.3^{ab}	1.9 ± 0.6^{bc}
Total		559.0 ± 78.6^{c}	1725.0 ± 125.0^{a}	1401.8 ± 218.5^{b}	1873.1 ± 167.8^{a}